



<http://www.diva-portal.org>

Preprint

This is the submitted version of a paper published in *Current inorganic chemistry*.

Citation for the original published paper (version of record):

Andersson, O., Yasuhiro, N. (2014)

Thermal Properties and Transition Behavior of Host –Guest Compounds under High Pressure.

*Current inorganic chemistry*, 4(1): 2-18

<http://dx.doi.org/10.2174/1877944104666140825201943>

Access to the published version may require subscription.

N.B. When citing this work, cite the original published paper.

Permanent link to this version:

<http://urn.kb.se/resolve?urn=urn:nbn:se:umu:diva-91799>

# **Thermal Properties and Transition Behavior of Host–Guest Compounds under High Pressure.**

Ove Andersson\*,† and Yasuhiro Nakazawa‡

†Department of Physics, Umeå University, 901 87 Umeå, Sweden

‡Research Center for Structural Thermodynamics, Graduate School of Science, Osaka University, Toyonaka, Osaka 560-0043, Japan

**Abstract:** The thermal properties and transition behavior of the host-guest inclusion compounds: urea, thiourea, Dianin's compound, clathrate hydrates and hydroquinone have been reviewed. In particular, we summarize their thermal conductivities, heat capacities and transitions at high pressures. Two of the systems: urea inclusion compounds and clathrate hydrates, show unusual glass-like thermal conductivity  $\kappa$ , i.e. their  $\kappa$  is low and only weakly dependent on temperature despite their crystalline structure. Moreover, results for  $\kappa$  of Dianin's compound with guests such as ethanol and  $\text{CCl}_4$  indicate a change from glass-like  $\kappa$  at atmospheric pressure to crystalline-like  $\kappa$  at elevated pressure, whereas  $\kappa$  of hydroquinone and thiourea inclusion compounds appears not to have been studied. Despite the technological and fundamental importance of the unusual glass-like  $\kappa$ , e.g. the use of inclusion compounds as structural model systems for finding improved thermoelectrical materials, the origin of the glass-like  $\kappa$  is not established. More specifically, the commonly employed rattling model, in which rattling guest motions cause resonance scattering of the acoustic host phonons, has recently been challenged, and we discuss alternative models. Heat capacity studies of these compounds reveal numerous transitions, which are associated with guest and host disorder-order transitions upon cooling and pressurization. A transition in hydroquinone may be of second order, or have only a small first-order component, which can explain discrepancies in the observed transition behavior. On pressurization at low temperatures, clathrate hydrates collapse to an amorphous state, which appears to be a glassy state of a water solution with perfectly spaced solute molecules.

**Keywords:** Glass-like behavior, Heat Capacity, High Pressure, Inclusion Compound, Phase Transition, Phase Diagram, Pressure Induced Amorphization, Thermal Conductivity, Structure, Glassy water solution.

## INTRODUCTION

### Host-guest compounds

There are a significant number of compounds that are referred to as “host-guest” compounds. [1] The classification into this type of compound is not always straightforward and sometimes somewhat arbitrary. This review of work done under high pressure is restricted to the subclass where the host forms a lattice with cages or channels, which can accommodate relatively weakly interacting guests. These host-guest species are commonly referred to as inclusion compounds or clathrates [1,2]. In the compounds, the guest and host molecules interact without strong ionic and covalent bonds and the guests are trapped in the framework formed by the host. We focus on five different compounds or classes of compounds: urea, thiourea, hydroquinone, ice clathrates and Dianin’s compound and the effect of direct or indirect guest-host interaction on their phase behavior and thermal properties, and specific features caused by high pressure densification. In particular, we review the effects on thermal conductivity, but we also present rare data for their heat capacity under pressure. Clathrates provide an ideal system for studies of atoms or molecules in nanometer sized cages, and several clathrates show unusually low and almost temperature independent thermal conductivity, which mimics that of glasses. Their common structural features have therefore been used as model for finding crystalline materials with low thermal conductivity, e.g. to identify potential materials for improved thermoelectrics, i.e. materials that generate a voltage when subjected to a temperature gradient, or *vice versa*. This bright idea proposed by Slack lead to the introduction of skutterudite thermoelectrics [3,4]. Moreover, as discussed in a detailed review by Struzhkin *et al.* [5], clathrates have also been suggested as candidate materials for hydrogen storage.

The properties of several of the selected compounds at atmospheric conditions have been discussed in the comprehensive book by Staveley and Parsonage [6], and the theory of clathrates has been reviewed by Belosludov *et al.* [7]. The thermal conductivity of clathrate hydrates have been discussed by English and Tse [8] and the transition behavior and heat capacity of numerous clathrate hydrates at atmospheric conditions have been reviewed by Yamamuro and Suga [9].

### Significance of high pressure studies

Application of high pressure provides a few important advantages compared to atmospheric pressure studies. In particular, high pressure helps in understanding material properties and may lead to new important technological materials. The most obvious effect of applying high pressure is strong densification of a material, which can occur without reduction of thermal energy. One can therefore derive the density dependence of a property. If the density dependence is independent of temperature, or only weakly dependent, the effects of changing volume in isobaric studies can be separated from other effects of changing temperature (thermal energy). One example, which is briefly discussed in this work, is the density dependence of the thermal conductivity, or the Bridgman parameter. With the aid of such data, it has been shown that the commonly observed change from a weakly positive temperature coefficient of the thermal conductivity below a glass transition to a negative coefficient above can be attributed entirely to the effect of changing density, or thermal expansivity, at the glass transition. However, most importantly, exposing a system to external pressure can introduce much larger changes in its Gibbs free energy than are possible with temperature. This gives potential access to a wide range of new materials with unknown chemical and physical properties. High pressure studies have also provided a new method to obtain amorphous materials, e.g. amorphous solid water [10], which have

furnished important results such as polyamorphism in water. This remarkable finding has subsequently been used as the basis for a new model of water's structure and unusual behavior [11]. But the increased complexity of measurements under high pressure limits the activity in this field. In particular, thermal property studies at high pressure are rare because these typically require large volume capacity, and this excludes the use of diamond and sapphire anvil cells. Despite relatively few studies, there are several extraordinary findings reported for the inclusion compounds discussed in this work.

### Thermal conductivity measurements

We here provide a brief account of a more extensive review of methods and theory used in high pressure thermal conductivity  $\kappa$  studies [12]. The general theory for  $\kappa$  is supplemented with the phenomenological model commonly used to account for the unusual glass-like  $\kappa$  of some inclusion compounds.

Measurements of  $\kappa$  under pressure are relatively rare but have an advantage that the risk of poor thermal contact between the probe and a solid sample is avoided. In the past, measurements were done using only steady-state methods, but these are subjected to relatively large uncertainties and are impractical for several reasons: (i) the dimensions of the sample must be determined, (ii) heat losses must be taken into account, and (iii) a static temperature gradient must be established, which may take up to an hour depending on the set-up. All these issues are resolved by using dynamic methods. There are various dynamic methods [13], and those which employ metallic heaters: e.g. hot-wires and hot-strips, have proven successful for high pressure studies up to a few GPa [14], whereas extreme pressures require methods based on diamond anvil cells [15]. Hot-wire methods are probably the most accurate, because hot-strip methods normally require substrates. These reduce the signal from the sample and their thermal properties must be determined, which increases the uncertainty. An additional advantage of dynamic methods is that these typically also give values for the heat capacity per unit volume, albeit with a rather large inaccuracy. In our studies, we have used the transient hot-wire method, but the theory of hot-strip methods is similar.

The hot-wire method is based on a solution of the time-dependent equation for heat conduction. The exact solution of the temperature rise  $\Delta T$  for an infinitely long, infinitely conducting wire immersed in an infinitely large specimen was derived by Carslaw and Jaeger [16]:

$$\Delta T = \frac{2q\alpha^2}{\pi^3\kappa} \int_0^\infty \frac{1 - \exp(-\beta u^2)}{u^3 \left\{ (u J_0(u) - \alpha J_1(u))^2 + (u Y_0(u) - \alpha Y_1(u))^2 \right\}} du, \quad (1)$$

where  $q$  is the constant heating power per unit length,  $\alpha = 2\rho c_p / (\rho_w c_w)$ ,  $\beta = \kappa t / (\rho c_p r^2)$ ,  $t$  is the time,  $r$  is the radius of the hot-wire,  $\rho$  and  $c_p$  are the density and specific heat capacity of the specimen,  $\rho_w$  and  $c_w$  are the density and specific heat capacity of the hot-wire,  $J_0$  and  $J_1$  are Bessel functions of the first kind of zero and first order,  $Y_0$  and  $Y_1$  are Bessel functions of the second kind of zero and first order.

The hot-wire probe used in high-pressure studies is typically made of a Ni alloy, which is both mechanically strong and has an electrical resistance that varies relatively strongly with temperature. This makes it well-suited for hot-wire experiments. The wire is mounted in a Teflon® sample cell for use as both heater and temperature sensor (Fig. 1). Due to the limited space available in the sample cell, and the requirement of a long hot-wire, the wire is placed in a ring of constant radius within the cell, and then immersed in the medium under investigation. To supply the load, hydraulic presses are used in combination with piston-cylinder type of pressure vessels, and

in some cases the whole set-up is enclosed in vacuum to avoid frosting in low-temperature investigations [17]. The values for  $\kappa$  and  $\rho c_p$  are obtained by fitting Eq. (1) to experimental values for the temperature rise of the hot-wire, which are measured simultaneously as the wire is heated with a short heating pulse. The inaccuracy is estimated as  $\pm 2\%$  in  $\kappa$  and  $\pm 5\%$  in  $\rho c_p$ . However, in the latter case, and sometimes for unclear reasons, we have occasionally observed larger deviations from more accurate methods. At low pressure, this can be due to poor thermal contact that strongly affects the initial part of the hot-wire temperature rise, which is most important to obtain accurate values for  $\rho c_p$ .

At phase and glass transitions, the hot-wire method gives anomalous results due to exothermic and endothermic heating and enthalpy relaxation, and these features are superimposed on real changes in  $\kappa$ . An endothermic transition occurring at an equilibrium phase line gives typically an anomalous peak in  $\kappa$ . This occurs when the enthalpy of the transition retards the transient heating of the hot-wire probe. The effect of a sluggish exothermic, non-equilibrium, transition on  $\kappa$  is more difficult to anticipate. Cold-crystallization gives a real increase in  $\kappa$ , which may be superimposed on an anomalous decrease caused by the heat evolution. In the vicinity of a glass-liquid transition,  $\kappa$  and  $\rho c_p$  often show an anomalous peak and dip, respectively. These arise because the heat capacity increases in a sigmoid shape manner on heating a glass through this range, and the change depend upon time, i.e. the heat capacity is time dependent on the time-scale of the measurements [18]. But in the fitting of Eq.(1) to the experimental data for the hot-wire temperature rise both fitting parameters,  $\kappa$  and  $\rho c_p$ , are treated as constants.

### The Debye model for thermal conductivity

Although we do not here use theory to fit the experimental data available in the literature, we still present the theoretical framework used in discussions of heat conductivity and the equations required for quantitative analyses. This outline also shows the importance of results obtained in high pressure studies for making the best comparison between theory and experimental results, and how the unusual glass-like  $\kappa$  reported for some of the inclusion compounds can be described by a phenomenological model, which originates from the picture of rattling guests in the cages of a host structure.

Results for  $\kappa$ , are often discussed in terms of the simple Debye formula [19]:

$$\kappa = \frac{1}{3} \rho c_V v \ell, \quad (2)$$

where  $\rho$  is the mass density,  $c_V$  is the specific heat capacity at constant volume,  $v$  is the phonon velocity and  $\ell$  is the phonon mean free path. This simplified equation is easily derived by assuming that the heat is carried by particles, phonons with a heat capacity per unit volume  $\rho c_V$ , that travel a distance  $\ell$  in between each collision.

Eq. (2) may be used to discuss  $\kappa$  of crystals at relatively high temperatures near the Debye temperature and above. Generally, the main carriers of heat are acoustic phonons and, at high temperatures, their heat capacity is roughly constant. The density and the phonon velocity decrease slightly with temperature, but normally the temperature change in  $\kappa$  is determined by the change in the phonon mean free path. In crystals, it is typically limited mainly by three phonon-phonon Umklapp scattering, i.e. processes where two phonons combine into a, new, third phonon with a wave vector outside the first Brillouin zone. The consequence is that the phonon momentum will not be conserved and the new phonon will move in a different, nearly opposite, direction than that suggested by the sum of the combined phonons' momentum, which explains the term "Umklapp" or flip-

over. At high temperatures, the number of phonons that can participate in Umklapp scattering processes increases in direct proportion to temperature. It follows that the mean free path varies inversely with temperature and, accordingly,  $\kappa$  as  $T^{-1}$ . This is also observed for many crystals and we here refer to it as crystalline-like  $\kappa$ . A stronger temperature dependence than this suggests that other, e.g. higher-order, phonon-phonon scattering processes become effective in limiting the mean free path and/or that the thermal expansion causes a significant decrease in  $\kappa$ . Slightly weaker temperature dependence indicates that structural scattering, such as scattering on grain boundaries, impurities and point defects, is also significant.

If instead the phonon mean free path in Eq. (2) is constant, e.g. due to lack of long-range structural order, then  $\kappa$  is governed by the weak changes in the three other parameters:  $\rho$ ,  $v$  and  $l$ . This is an assumption which may be done to understand the behavior of liquids and glasses at high temperatures. In the case of an amorphous state, the disordered structure does not allow for long-range phonon propagation, at least not for high frequency excitations. Therefore the concept of phonons in glasses and the use of Eq. (2) might be disputed. However, the equation should be applicable for samples in which the crystal sizes are small enough to make boundary scattering the dominant scattering source. In these cases,  $l$  would become small and almost independent of temperature, which is the behavior observed for glasses, and it is here referred to as glass-like  $\kappa$ .

At a glass transition temperature,  $T_g$ , experimental results show that the temperature derivative of  $\kappa$  ( $d\kappa/dT$ ) typically changes from small and positive to small and negative. If  $l$  is constant in Eq. (2), then a positive  $d\kappa/dT$  must be due to an increasing heat capacity, because  $v$  and  $\rho$  normally decrease with temperature. The change to a negative value at  $T_g$  can be described quantitatively by Eq. (2) through the increase in the thermal expansivity which decreases the density [20].

A constant mean free path, explains the weak temperature independent  $\kappa$  of glasses and liquids, but also a few cases of well-ordered crystals show deviant behavior from crystalline-like  $\kappa$ . In particular, clathrates take a prominent place among crystalline systems that show glass-like  $\kappa$ . This unusual feature was first observed for ice clathrates [21] and lead to the “rattling”, or resonance scattering, model where rattling guest motions are assumed to strongly scatter phonons, as suggested by Tse and White [22], and Slack and co-workers [3, 23]. Although support for the model has been presented [24], it was recently challenged, at least for the cases of La- and Ce-filled  $\text{Fe}_4\text{Sb}_{12}$  [25] and  $\text{Ba}_8\text{Ga}_{16}\text{Ge}_{30}$  (type I clathrate) [26].

Eq. (2) can also be used to understand the change of  $\kappa$  of crystals at an isothermal increase of pressure. Isothermal densification typically increases the Debye temperature, which decreases the heat capacity. With only a few exceptions, all the other parameters in Eq. (2) ( $\rho$ ,  $v$ ,  $l$ ) increase. The density must increase at increasing pressure and this normally leads to increasing phonon velocity. (In e.g. ice, however, the transverse sound velocity decreases.) When the Debye temperature increases then the number of phonons that can participate in Umklapp processes also decreases, which leads to a slight increase of the mean free path. Moreover, normally the lattice becomes more harmonic when pressure is applied, i.e. the Grüneisen parameter ( $=d \ln v/d \ln \rho$ , where  $v$  is the phonon frequency) decreases. As a result, the coupling constant between phonons, which is typically proportional to the square of the Grüneisen parameter [27], decreases and this leads to less frequent phonon scattering. Thus, Eq. (2) predicts that  $\kappa$  of crystals should increase with pressure, which is also almost invariably observed in experiments. For glasses and liquids, the change of  $\kappa$  with pressure is again governed by the changes of:  $c_V$ ,  $\rho$ , and  $v$  since the mean free path remains about constant. As for crystals,  $c_V$

may decrease slightly but the increase of  $\rho$  and  $v$  more than well compensate for this decrease, and  $\kappa$  should increase. This behavior has also been observed for all liquids and glasses with only one exception, the low density amorphous state of ice [28].

The Debye formula described by Eq. (2) can be used in qualitative and simple quantitative comparisons between theory and experimental results at temperatures higher than the Debye temperature. However, in a more realistic comparison it is necessary to take into account the frequency dependence of scattering processes, especially at low temperatures. This includes the range where Umklapp scattering ceases because of a vanishing number of phonons with wave vectors near the limit of the first Brillouin zone. As a consequence, the relative importance of scattering processes due to defects increases. Under these conditions, it is common to calculate a relaxation time for each phonon frequency, and the equation becomes [29]:

$$\kappa = \frac{k_B^4 T^3}{2v\pi^2 \hbar^3} \int_0^{\theta_D/T} \tau(x) \frac{x^4 e^x}{(e^x - 1)^2} dx ; \quad x = \frac{\hbar\omega}{k_B T} \quad (3)$$

where  $\theta_D$  is the Debye temperature,  $\tau(x)$  is the resultant relaxation time,  $\omega$  is the phonon angular frequency and the other symbols have their usual meanings. A requirement for the validity of Eq. (3) is that the redistribution of phonons by normal phonon-phonon processes and its (indirect) contribution to the thermal resistivity can be ignored. Moreover, in the form given here, no distinction is made between transverse and longitudinal modes other than that the phonon velocity can be calculated as a weighted average of the modes.

The relaxation time for three-phonon Umklapp processes has been written in various forms, but one of the most common form used at  $T \leq \theta_D$  is given by [29,30]:

$$\tau_u^{-1}(x) = A x^2 T^3 e^{-\left(\frac{\theta_D}{\beta T}\right)} \quad (4)$$

where  $A$  is the scattering strength for three-phonon Umklapp scattering and  $\beta$  is a constant. To account for scattering processes associated with structural defects, e.g. point defects, boundaries etc., additional terms must be included [29,30]. Moreover, it has been suggested that the rattling of guest molecules in clathrates can give rise to strong phonon resonance scattering, i.e. the rattling model, and various scattering terms have been derived to account for this effect. Adding these terms together typically gives a total relaxation time:

$$\tau^{-1}(x) = A x^2 T^3 e^{-\left(\frac{\theta_D}{\beta T}\right)} + B x^4 T^4 + \frac{v}{C} + N_0 D \frac{\omega_0^2 \omega^2}{(\omega_0^2 - \omega^2)^2} \quad (5)$$

where  $B$  and  $C$  are constants which normally are associated with point defect and boundary scattering, respectively [29,30]. The last term is a phenomenological expression used to account for resonance scattering when it is associated with a single (rattling) frequency  $\omega_0$  [22].  $N_0$  is the concentration of resonance scatters, or guests, and  $D$  is a coefficient describing the coupling strength between phonons and guest vibrations.

Also other scattering terms may be included, but at moderately high temperatures ( $\sim \theta_D$ ), there is a relatively small difference in the temperature dependence of  $\kappa$  between cases where the dominating scattering processes differ only weakly in phonon frequency dependence. For example, scattering from strain fields of dislocations ( $\tau^{-1} \propto \omega$ ) [29,30] yields about the same dependence as one governed by a constant relaxation time, i.e. the same as for boundary scattering. Thus, the results discussed in this review, which typically concerns

temperature above 50 K, can be described by a total relaxation time of the form given by Eq. (5). Under such conditions, the point defect and boundary scattering terms in Eq. (5) can also roughly account for scattering processes which have slightly different dependence on phonon frequency.

The theory described by Eqs. (2) and (3) assumes that the sample volume is constant, i.e. these do not take into account changes in  $\kappa$  due to thermal expansion. Consequently, to make a quantitative comparison between theory and experimental results, the measured isobaric data should be transformed to isochoric conditions. This requires measurements of  $\kappa$  when the sample is densified under isothermal conditions, and shows one major importance to employ high pressure in these studies.

The change in  $\kappa$  due to expansion alone is given by [20, 31]

$$\left(\frac{\partial \ln \kappa}{\partial T}\right)_p - \left(\frac{\partial \ln \kappa}{\partial T}\right)_\rho = -\alpha \cdot g \quad (6)$$

where  $g (= \partial \ln \kappa / \partial \ln \rho)_T$  is the Bridgman parameter and  $\alpha$  is the volume thermal expansivity. Consequently, data for both thermal conductivity and density as a function of pressure are required for employing Eq. (6).

### Heat capacity measurements

Heat capacity investigations under high pressure are probably even rarer than thermal conductivity studies. High accuracy methods such as adiabatic calorimetry have poor compatibility with the need to apply high pressure. Yet some have used gas pressure in combination with adiabatic cells and pressures up to about 0.25 GPa have been reached [32]. But to obtain very high pressures clamped cells must be used [33]. In this case, a limitation is that the pressure cannot easily be changed other than at room temperature, and it can also not be kept constant as the cell and sample volume changes on heating and cooling. Non-adiabatic methods are less accurate but better suited for high-pressure studies. Most common are methods based on metal heaters in combination with piston-cylinder apparatuses or multi-anvil cells [34]. One of these is the hot-wire method, which is describe above, and others are based on thin-film heaters that are placed (evaporated) onto a substrate or directly on a (solid) sample. The draw-back of the latter technique is that the thermal properties of the substrate, or those of the pressure transmitting medium, must be subtracted. Moreover, a general problem with dynamic methods is that they typically give the heat capacity per unit volume (i.e. the density must be known to obtain the heat capacity per unit mass) or the thermal diffusivity, which requires the thermal conductivity. (The hot-wire method gives both  $\kappa$  and  $\rho c_p$ .) More recently, methods based on laser heating in diamond cells have been developed, and these permits studies at very high pressures of up to at least 20 GPa [15,35].

In studies of inclusion compounds, the use of a gas to apply pressure provides the great advantage of, *in-situ*, production of gas clathrates. That is, the gas system can both be used to study the effect of pressure on transitions and heat capacity and to produce the clathrate sample. Yamamuro *et al.* [32] used their high-pressure system to obtain high-accuracy heat capacity data for Ar clathrate hydrate. This is one of few high-accuracy studies of the heat capacity for clathrate hydrates under pressure. It showed that their assumption of an ice host lattice with the same heat capacity as hexagonal ice, and an excess heat capacity due to that of the guest, reproduced “fairly well the experimental data”. Using a simple one dimensional Pöschl-Teller potential for the potential wells of the Ar atoms, with two free parameters; the diameter of the clathrate cages and the stiffness, the model suggested cage sizes of 2.2 Å and 3.8 Å for the D and H-cages, respectively, which are less than their actual sizes (7.8 Å and 9.4 Å –see section about clathrate hydrates). However, Yamamuro and Suga [9] also

concluded that the same assumptions for Xe and Kr clathrate hydrates could not describe well the experimental data.

## TRANSITION BEHAVIOUR AND THERMAL PROPERTIES UNDER PRESSURE

### Hydroquinone

Hydroquinone (HQ) can exist in three different crystalline forms under atmospheric pressure conditions:  $\alpha$ ,  $\beta$  and  $\gamma$ . The stable ambient phase of pure HQ, i.e. without guests, is the  $\alpha$ -form, where HQ crystallizes in the rhombohedral space group  $R\bar{3}$  with 54 molecules in each unit cell of hexagonal dimensions:  $a = b = 38.46(2)$  Å,  $c = 5.650(3)$  Å and a density of  $1.36$  g cm<sup>-3</sup> [36]. Both the  $\beta$ - and  $\gamma$ -forms are metastable under ambient conditions. The latter, which is monoclinic,  $P2_1/c$ ,  $a = 8.07$ ,  $b = 5.20$ ,  $c = 13.20$  Å,  $\beta = 107^\circ$  with 4 molecules per unit cell and a calculated density of  $1.380$  g cm<sup>-3</sup> [37], can be produced by sublimation of a solution in ether. The  $\beta$ -form is typically obtained in association with clathrate formation, but may remain metastable even if the guest species are removed by heating. The  $\beta$ -form shows a hexagonal structure,  $a = 16.61$  Å and  $c = 5.511$  Å (space group  $R3$ ), with methanol guests [38], and commonly roughly similar values for  $a$  and  $c$  for the  $\beta$ -form with other guest species, e.g. HCl, HBr, H<sub>2</sub>S, C<sub>2</sub>H<sub>2</sub> and SO<sub>2</sub> [39, 40]. The “empty”  $\beta$ -form, i.e. without guest molecules, has a density of  $1.258$  g cm<sup>-3</sup> [41].

Yet another form of HQ, the  $\delta$ -form, has been detected at elevated temperatures and pressures by Naoki *et al.* [42]. In their differential thermal analysis (DTA) and volume measurements, they observed an endothermic transition from the  $\alpha$ -form to a slightly denser phase ( $1.355$  g cm<sup>-3</sup> at  $443.3$  K and  $78.5$  MPa) on isobaric heating above  $0.03$  GPa. Naoki *et al.* [42] used their DTA and volume results under pressure together with atmospheric pressure results to calculate the high pressure properties of the  $\delta$ -form from thermodynamic relations. The temperature-pressure  $T$ - $p$  phase line between the  $\alpha$ -form and the new  $\delta$ -form has a negative slope, as shown in Fig. 2. Accordingly, the  $\delta$ -form has higher entropy and they also derived a significantly higher molar heat capacity for the  $\delta$ -form than that of the  $\alpha$ -form. The heat capacity of the  $\delta$ -form is close to that of the liquid, which Naoki *et al.* attributed to “rigid body vibrations and/or librations”. Another possibility could be that the  $\delta$ -form has some degree of rotational freedom. However, the  $\delta$ -form is far from fulfilling the entropy definition of a plastic crystal, i.e. a crystal with a significant degree of rotational freedom. In terms of Timmermann’s definition [6,43], a plastic crystal shows an entropy of fusion of less than  $5R/2$ , where  $R$  is the gas constant. Although the  $\delta$ -form has a large molar heat capacity close to that of the liquid their entropies differ more than  $6R$  [42].

Subsequently, the  $\alpha$ -form of HQ was also studied by Rao *et al.* [44] using Raman spectroscopy under high pressure. During isothermal pressurization in a diamond anvil cell at room temperature, they observed changes in the Raman spectra suggesting two transitions at  $3.3$  GPa and  $12$  GPa, respectively. The  $3.3$  GPa feature was attributed to a new phase, but considering the results of Naoki *et al.* [42], it may correspond to the  $\alpha$  to  $\delta$  transition, which they observed at lower pressures and high temperatures. The transition line obtained by a linear extrapolation of Naoki *et al.*’s data intersects the room temperature isotherm at  $1.7$  GPa, i.e. significantly below  $3.3$  GPa. However, due to the limited pressure range of Naoki *et al.*’s study (below  $0.1$  GPa), this can be accounted for by the uncertainty of the extrapolation in combination with significant pressure inaccuracy in diamond anvil cells. In the phase diagram in Fig. 2, hypothetical phase lines have been inserted assuming that the

two phases are identical. Rao *et al.* [44] found that the 3.3 GPa transition was reversible upon pressure decrease, but with a significant pressure hysteresis, and the ambient pressure phase was recovered below 1.3 GPa. Rao *et al.* [44] hypothesized that the transition is a group-subgroup transition involving loss of inversion symmetry, e.g. a *trans-cis* conformational change. The results of Naoki *et al.* [42] show that their  $\alpha$  to  $\delta$  transition is a first-order transition but with only a small volume change of about 1%. As mentioned, the changes in heat capacity and thermal expansion coefficient are, however, large. Consequently, by studying any of these properties, it should be possible to map the transition line up to higher pressures and investigate whether or not the new phase suggested by Rao *et al.* is identical to that studied by Naoki *et al.*

Rao *et al.* [44] noted that the transition at 12 GPa is associated with an extensive broadening of the Raman lines caused by an increasing disorder, and they suggested that this is due to a hindered transition to a  $\gamma$ -hydroquinone-like structure. They discussed this feature in terms of pressure induced amorphization into an amorphous-like structure that occurs in some hydrogen-bonded systems such as ice, which is the most well-known example [10]. It has been suggested that the pressure induced transition from hexagonal ice to amorphous ice occurs due to a mechanical instability of the crystalline hexagonal ice phase [45]. This instability forces a transformation into a denser phase, and the thermodynamically most stable phase is typically another crystalline phase (ice VI). However, for kinetic reasons, this transition is obstructed and when the crystalline phase becomes mechanically unstable, it instead collapses to an amorphous state. The work of Rao *et al.* [44] suggests that something similar may occur for HQ at 12 GPa. However, Rao *et al.* [44] also noted that “nonhydrostatic effects start increasing beyond pressures of about 11 GPa”, which provide an alternative explanation for the observed broadening of the Raman lines. Although, this work does not provide indisputable evidence for pressure induced amorphization in a clathrate system, such evidence exists for ice clathrates, which is discussed further below.

In two recent studies, Yoon and coworkers [46,47] investigated both the  $\beta$ -form, with and without a guests ( $N_2$  and  $CH_4$ ), and the  $\alpha$ -form of HQ under high pressure conditions. They studied the structural changes at room temperature using synchrotron X-ray scattering and Raman spectroscopy but found no evidence for a transition in the  $\alpha$ -form up to 8.8 GPa, despite the report of a transition near 3 GPa [44] and the well-established  $\alpha$  to  $\delta$  phase line at high temperatures, which also suggests a transition upon isothermal pressurization at room temperature [42]. Although the transition at elevated temperatures and pressures is a first-order transition, the lack of features of Yoon and coworkers’ [46,47] X-ray spectra suggests that any transition at room temperature must be of second-order, or have only a weak first-order component.

Yoon and coworkers’ study of the  $\beta$ -form shows that the empty lattice transforms irreversibly into the stable  $\alpha$ -form at 0.4 GPa, which thus remains stable upon pressure release. The  $N_2$  or  $CH_4$  loaded  $\beta$ -form shows a structural transition at 4 GPa and 5 GPa, respectively, which causes a gradual release of  $N_2$  from the clathrate structure on further pressure increase. This transformation is reversible and the original  $\beta$ -structure is thus recovered upon pressure decrease.

HQ with guests such as HCN and methanol also shows an interesting transition on cooling at ambient pressures. Matsuo and coworkers [48,49] used adiabatic calorimetry and dielectric measurements and revealed ordering transitions at 177.8 K in the HCN clathrate, and in the range 44.4 K to 65.7 K in the methanol clathrate depending on the methanol occupation fraction, which varied from 0.728 to 0.974. They concluded that these transitions are due to orientational ordering transition of the guest molecules.

In the case of HQ, one can conclude that two studies suggest a transformation in the  $\alpha$ -form upon pressure increase, but that this is not well-established and require further studies because of lack of features in structural studies. There seems to be no investigations of thermal properties under high pressure conditions other than that of Naoki *et al.* [42], which concerned pressures below 0.1 GPa. But considering the large difference in the heat capacity between the  $\alpha$ - and  $\delta$ -forms, such a study would probably be rewarding and would likely resolve the issue concerning a possible  $\alpha$  to  $\delta$  transformation on isothermal pressurization at room temperature.

### Urea and thiourea

Urea, which is also referred to as carbamide, has the chemical formula  $\text{CO}(\text{NH}_2)_2$ . Thiourea is the sulfur analog of urea and has, accordingly, the chemical formula  $\text{CS}(\text{NH}_2)_2$ . The fundamental properties of both urea and thiourea and their inclusion compounds have been reviewed by Harris [50].

The phase diagram of urea for pressures up to 1 GPa and temperatures in the range 271-430 K, shown in Fig. 3, was established by Bridgman [51,52]. Bridgman used volume measurements and reported three solid phases: phase I, II and III, where phase II is stable at pressures above about 0.65 GPa and temperatures above 375 K (Fig. 3). Subsequently, Hamann and Linton [53] used infrared measurements at room temperatures and verified the existence of phase III. More recently, urea has been studied at room temperature at even higher pressures, and two new phases were reported: Phase III transforms into phase IV at about 2.8 GPa and further to phase V at 7.2 GPa [54,55].

Urea crystallizes in a tetragonal lattice,  $P\bar{4}2_1m$  [56] (Phase I). The structure of phase II is unknown but phases III and IV have been studied in detail and these are both orthorhombic with space group  $P2_12_12_1$  [54,55,57]. Phase V has been suggested to be orthorhombic with space group  $Pmcn$  [54,55].

At atmospheric pressure, phase I is stable, or metastable, from the freezing point down to low temperatures. No transition to a more ordered low-temperature modification has been established, but there are a few reports of features indicating a constrained transition on cooling below room temperature [58]. Moreover, the phase diagram suggests that phase I can be metastable below 218 K [59], still adiabatic heat capacity results provide negative evidence for a transition [60]. Thus, urea can be among the quite a few cases for which a transition to a phase with the lowest Gibbs energy is obstructed for kinetic reasons. One of the most famous case is hexagonal ice, which remains stable down to 0 K despite that proton-ordered phase, ice XI, is the thermodynamically stable state [61]. The latter can only be obtained after suitable doping, e.g. with KOH, which relaxes the ice rules [62] that restricts proton movements and a transition into the proton ordered ice phase XI. The phase diagram of urea suggests that a transition from phase I to phase III should occur at about 220 K on cooling at low pressures and, thus, that phase III is the thermodynamically stable phase below 220 K at atmospheric pressure.

A study of the thermal properties of urea [59] shows that phase III has about 20% lower  $\kappa$  than phase I (Fig. 4), despite its 7% higher density [63]. A decrease in  $\kappa$  at a pressure induced transition is rather unusual but it has been observed before, e.g. for KBr [64]. In the case of KBr, the transition was sluggish, which also was the case for urea at low temperatures. This is shown by the wider transition range at 252 K compared to that at 295 K (Fig. 4a and 4b). From the temperature dependence of  $\kappa$  (Fig. 4d), it was deduced that three-phonon Umklapp scattering was the dominant scattering process in both phases I and III of urea [59]. In terms of the simple Debye formula, Eq. (2), the significant difference in the magnitude should therefore be due to a stronger scattering strength (shorter  $l$ ) and/or lower phonon velocity in phase III. The recent comprehensive study of the phase I and

III structures [57] provides further information concerning the unusual decrease of  $\kappa$  at the transition to the high-density phase III. Based on their structural analysis, Olejniczak *et al.* [57] established a major change in the hydrogen-bonded network at the phase I to phase III transition. In particular, some hydrogen bonds break and the dimensions of others change significantly. In phase I, each molecule forms eight hydrogen bonds, but only six in phase III. Thus, this drastic change in the hydrogen bonded network may explain the unusual decrease in  $\kappa$ .

The heat capacity per unit volume of urea, show the typical behavior of molecular solids. That is, it increases with increasing pressure, and decreases with decreasing temperature (Fig. 4). At equilibrium phase transitions, the measurement method used in this study, the hot-wire method (see above), gives anomalous results because of the heat of transformation. But the results above and below this range, suggest that  $\rho c_p$  is almost continuous through the transition. At low pressures, ca. 0.15 GPa, the derivative of  $\rho c_p$  changes discontinuously (Fig. 4a). Concurrently,  $\kappa$  shows a small dip (Fig. 4b), which provides weak indications of a higher-order transition, e.g. a freezing of a molecular motion. If this is indeed the case, then the transition is almost independent of temperature. However, there are no other reports that suggest a transition in this pressure range.

If we turn to the inclusion compounds of urea, then the most common structure is hexagonal with  $a \approx 8.2 \text{ \AA}$  and  $c \approx 11.0 \text{ \AA}$  and space group  $P6_122$  or  $P6_522$  [65,66]. The urea molecules form a hollow channel structure with linear parallel tunnels that, e.g., n-hydrocarbon molecules can accommodate. The periodicity of the urea host and the periodicity of the guest are normally incommensurate along the channel axis. At high temperatures, the guest may be relatively mobile and reorient, but as the temperature is lowered, the reorientation typically ceases at an ordering transition, which is also accompanied by a change in the structure. Toudic *et al.* [67] have studied the phase behavior and structures of deuterated urea-nondecane inclusion compound under pressure, and they suggested the phase diagram shown in Fig. 5. They observed four phases and reported that “All the phases (I, II, III, IV) require a description within a crystallographic superspace: hexagonal for the phase I, orthorhombic for the phases II, III and IV.” This appears to be one of few structural studies of urea inclusion compounds under pressure. Unfortunately,  $\kappa$  and  $c_p$  of urea-nondecane inclusion compound have not been studied. Ross has, however, measured  $\kappa$  of urea-hexadecane inclusion compound [68]. Ross measured  $\kappa$  at 0.1 GPa pressure and reported indications of a phase transition at 160 K (see Fig. 6), in agreement with results of an earlier heat capacity study by Pemberton and Parsonage [69]. Moreover, Ross noted that  $\kappa$  of the high temperature phase was independent of temperature and that  $\kappa$  of the low temperature phase decreased only weakly with temperature. These behaviors are far from the  $T^{-1}$  behavior commonly found for ordered crystals. In Fig. 6b, the results for the urea-hexadecane compound are plotted against temperature at 0.1 GPa, together with results for (metastable) phase I of urea at 0.28 GPa. The difference is striking as the latter shows typical crystalline-like  $\kappa$ , whereas the inclusion compound show glass-like  $\kappa$ . This was not the first crystalline material that had shown such deviant behavior. As noted above, Ross and coworkers [21] first discovered this in ice clathrates, which was a remarkable finding. It was initially attributed to the orientational reorientation of the guests, which was a logical conjecture since  $\kappa$  of many orientationally disordered phases, both in frozen states (glassy crystals) and in unfrozen states (e.g. plastic crystals), show similar behavior as that of liquids and glasses [64,70]. But since also ice clathrates with monoatomic guests show glass-like behavior at temperatures above 100 K [71,72], this cannot be the origin for the weak temperature dependence of  $\kappa$ . The weak temperature dependence can, however, be semi-quantitatively described by the phenomenological model, which attributes the weak  $\kappa(T)$  to resonance scattering (see Eq. (5)) [22].

If we consider thiourea, then the phase diagram depicted in Fig 7 shows a more complex transition behavior than that of urea. At room temperature, thiourea crystallizes in an orthorhombic lattice in space group Pbnm with  $a=5.488$ ,  $b=7.663$  and  $c=8.564$  Å and shows a closely-packed hydrogen bonded structure. The phase (phase V) is paraelectric but transforms to a ferroelectric phase (phase I,  $Pb2_1m$ ,  $Z=4$ ) at 202 K, via several intermediate higher-order transitions. The phase diagram has been the subject in several studies [52,73,74,75] and the one depicted in Fig. 7 is based on a summary made by Gesi [74].

The thermal conductivity of a single crystal of thiourea has been studied by Menon and Philip [76] using a photopyroelectric technique (Fig. 8). Their results indicate a crystalline-like  $\kappa$ , which is similar to the behavior of urea. However, the magnitude at room temperature is about  $100 \text{ W m}^{-1} \text{ K}^{-1}$  in thiourea and  $1 \text{ W m}^{-1} \text{ K}^{-1}$  in urea [59], i.e. about 100 times larger in thiourea, which is a surprisingly large difference. In principle this could be due to the use of a single crystal instead of a polycrystalline material, but normally the difference between single crystal and polycrystalline materials is not a factor of 100, at least not near room temperature. Moreover, there is no reason that  $\kappa$  of thiourea should be much larger than that of urea. Urea shows a magnitude of  $\kappa$ , which is typical of an organic crystal. (This could mean that there is a mistake in the unit of figure 5 of Ref. [76].)

We have not found any studies of  $\kappa$  or  $c_p$  of thiourea inclusion compounds under pressure. In fact, we found only a few studies of the high pressure properties of thiourea inclusion compounds. However, the phase diagrams of two thiourea inclusion compounds, which form ferroelectric phases, have been studied by Bilski and co-workers [77, 78]. Despite the similarity between the compounds, the phase diagrams, which are depicted in Fig. 9, differ significantly. In particular, bis-thiourea pyridinium bromide shows extensive polymorphism, which suggests that a study of the thermal properties would be interesting to determine the effect of structural changes. Since the tunnels in the thiourea host structure are larger in cross-sectional area than those in the urea host structure [66], it can accommodate larger guest molecules and, thus, it provides also a further opportunity to study the effect varying guest molecules on  $\kappa$ .

### Dianin's compound

Dianin's compound [4-(*p*-hydroxyphenyl)-2,2,4-trimethylchroman] is special among the guest-host compounds since it forms both clathrates and an isostructural form that is stable without guests. Dianin's compound can accommodate numerous guest molecules such as  $\text{CCl}_4$  [79] and ethanol [80], and the guest-free compound crystallizes in the trigonal space group  $\bar{R}3$  with  $a= 26.965$  Å and  $c= 10.933$  Å [81]. In a recent comprehensive structural study, Lee *et al.* [82] have reported the structure of 18 of its clathrates, as well as data on the location, orientation and dynamics of the guests in the host cavity. They concluded that "Although all unit cells are closely similar in size, the host undergoes significant change in response to the imprisonment of its various guests.", i.e. structural analysis of each clathrate may be required to understand differences in their properties.

We have been unable to find any studies of the  $p$ - $T$  diagram of Dianin's compound. In fact, there are relatively few studies of this compound, and only one of these has concerned high pressure. It reported the thermal properties of Dianin's compound and its ethanol and  $\text{CCl}_4$  clathrates [83], and the results are shown in Fig. 10.

The data for  $\rho c_p$  of the compound without guests as well as with ethanol or  $\text{CCl}_4$  guests measured on cooling at 0.2 GPa are depicted in Fig. 10a. As shown,  $\rho c_p$  decrease smoothly with decreasing temperature. That is, these

data suggest that there is no transition on cooling down to about 50 K at 0.2 GPa. Moreover, the data indicate that  $\rho c_p$  of the compound with guests is slightly higher than that without. Since the structure is essentially unchanged, the inclusion of guests increase the density, and likely also the heat capacity.

The  $\kappa$  of single crystal and polycrystalline material of Dianin's compound, and its ethanol and  $\text{CCl}_4$  clathrates was studied by White and co-workers [83,84,85]. They used both the hot-wire method and a steady-state radial heat flow method to study the behavior at high pressure [83], and a modulated heat flow method to study the behavior at atmospheric pressure [84,85,86]. All high pressure results, independent of sample (empty or filled Dianin's compound) and method (hot-wire or radial heat flow method) showed crystalline-like behavior, whereas the atmospheric pressure data showed glass-like behavior irrespectively of sample: empty or filled, polycrystalline or single crystal Dianin's compound [84,85]. Consequently, these results suggest a change from the unusual glass-like  $\kappa$  at atmospheric pressure to normal crystalline-like dependence of  $\kappa$  under elevated pressures. The reason for such change should be due to: (i) a strong pressure induced shift in the vibrational frequency of some scattering source, (ii) a strong shift in the frequency of the dominant heat carrying modes, or (iii) a phase transition, unless there are systematic errors in either the high or atmospheric pressure measurements. The first possibility (i), which would provide support for the rattling, or resonance scattering, model [24], was further studied by Raman measurements under pressure [83]. Although several candidates for a strong scattering source were found, no-one showed a Raman peak that shifted significantly with pressure. Consequently, either there is no such rattling mode that causes the glass-like behavior observed at atmospheric pressure, or it occurs below the range covered by the Raman study (i.e. below  $70 \text{ cm}^{-1}$ ), which is, in fact, the most likely range for a rattling mode. Another possibility that would be consistent with the resonance scattering model [24] is that the dominant heat carrying modes are instead strongly shifted by pressure, i.e. case (ii), and therefore moved off resonance of a strong phonon scattering source. To fully rule out, or establish, any of the possibilities (i) and (ii) would require inelastic x-ray and/or neutron scattering studies under pressure. However, if we consider the glass-like results for the compound without guests at atmospheric pressure [84], then these are obviously not compatible with the original rattling model where the rattlers are associated with the guest molecules. Zakrzewski and White [84] therefore suggested that also the host methyl groups could serve as strong resonance scatters and take the role of the rattlers in the clathrate without guests. The third possibility that can cause a significant change in  $\kappa$  behavior under pressure is a phase transition (iii). However, since the high-pressure results showed crystalline-like  $\kappa$  down to relatively low pressures (about 0.035 GPa), it means that such a transition must occur at even lower pressures. This issue was difficult to study in the measurements of the thermal properties because good thermal contact with the probe cannot be ensured below 0.05 GPa. It would, however, be somewhat surprising if such low pressure, or densification, would cause a phase transition irrespectively whether or not the cages are filled.

Indications of a transition in Dianin's compound was indeed observed but then at much higher pressure. Fig. 11 shows results on initial pressurization of Dianin's compound with  $\text{CCl}_4$  guests at room temperature. The rather strong initial increase of both  $\kappa$  and  $\rho c_p$  is typical when a virgin powdered material is compacted at the initial pressure increase. Although the results in  $\kappa$  do not indicate any strong features on pressure increase, the results for  $\rho c_p$  show a dip at about 0.7 GPa, which may be due to a transition. This pressure is, however, rather close to the phase II to III transition in Teflon at about 0.65 GPa at 295 K [87]. Since Teflon is the material which is used in the sample cell, this may be the cause of the subtle effects noticed in the data. In any case, this

possible transition cannot explain the crystalline-like temperature dependence of  $\kappa$ , which is observed already at pressures near 0.035 GPa.

We can conclude that the studies of White and co-workers [83,84,85] could not verify the resonance scattering model, or establish some other origin for the glass-like  $\kappa$  observed in inclusion compounds. However, the results suggest that further studies, and particularly high-pressure studies, of Dianin's compound may be helpful to establish the origin of the unusual feature. The fact that a change to crystalline-like behavior occurs already at about 0.035 GPa (350 bar), or less, means that the range can be relatively easily studied by numerous methods. The glass-like results for Dianin's compound both with and without guests at atmospheric pressure suggest that it is not the guests that are the main origin of glass-like  $\kappa$ , but instead the structure. This is in correspondence with the model by Dharma-wardana [88]. He studied clathrate hydrates and suggested that the glass-like behavior for  $\kappa$  of clathrate hydrates is due to the large number of atoms per unit cell, which gives numerous optical phonon modes. Typically, optical phonons have flat dispersion relations, i.e. low velocity, which limits their contribution to heat transport. The model of Dharma-wardana suggests that optical phonons cause strong scattering of acoustic phonons, and therefore limit their mean free path to the same extent as occurs in glasses and liquids due to structural disorder. This model cannot, however, explain glass-like  $\kappa$  in all crystalline materials, e.g.  $\text{Sn}_2\text{P}_2\text{S}_6$  [89] in which the number atoms in the unit cell do not change at a ferroelectric to paraelectric phase transition, yet the paraelectric phase shows glass-like behavior whereas the ferroelectric phase shows crystalline-like behavior. Moreover, in order for the model to be consistent with the pressure induced change in the behavior of  $\kappa(T)$  of Dianin's compound, then a structural transition must occur on pressurization to 0.035 GPa.

### **Clathrate hydrates**

Clathrate hydrates (CHs), or ice clathrates, are inclusion compounds in which the host, water, forms cages which accommodate various guest molecules [90,91]. Without the guests, the structure is unstable. Hydrocarbon filled CHs exist naturally in large amounts in permafrost, and in the deep ocean floor, and are at the same time potentially both an energy source and an environmental threat. This is one reason for the great interest in the CHs' properties, and in particular their thermal properties, but there are several more reasons to analyze and investigate CHs.

In a pioneering study, Ross *et al.* [21] were first to show that the temperature dependence of  $\kappa$  of an inclusion compound, tetrahydrofuran (THF) CH, was similar to that of glasses. Later, this was shown to be a general feature of CHs. This remarkable deviation from crystalline-like behavior for a polycrystalline material still attracts a lot of attention because its origin is important for the search of better materials in applications that require crystalline materials with poor  $\kappa$ . Yet, more than 30 years after Ross *et al.*'s discovery, the reason for the glass-like  $\kappa$  is not established [25,26]. The result of Ross *et al.* inspired Slack and co-workers [3,23] to suggest similar, but electrically conducting, materials, to optimize the figure of merit of thermoelectric materials. The thermoelectric effect is the phenomenon by which an electric potential difference develops in a circuit due to a temperature gradient, or the reverse, and the figure of merit is proportional to the electrical conductivity but inversely proportional to  $\kappa$ . Slack and co-workers combined the finding of Ross *et al.*, and Slack's concept of minimum  $\kappa$  [92], and coined the idea of a phonon-glass electrical-crystal to find the best thermoelectric

materials. Thus, the surprise finding of Ross *et al.* [21] was likely the start of the new methodology for search for better thermoelectric materials and lead to the introduction of skutterudite thermoelectrics.

In another important study, Suzuki [93] showed that THF CH collapsed to an amorphous state in a similar manner as ice on pressurization at low temperature [10]. This work followed Ross and Andersson's studies [94,95] that reported indications for a transition in THF CH on pressurization at 130 K, and Handa *et al.*'s volume study [96] that suggested a transition to an amorphous state on pressurization of the same material at 77 K. This finding is important to understand the phenomenon of pressure induced amorphization, but may also help to understand the reason for, and properties of, the multiple amorphous states of water [10, 97, 98].

CHs typically crystallize in one of three structures denoted: I, II, and H. The two former have cubic space groups Pm3n and Fd3m, respectively, and are the most common [90,91]. (The H-structure is hexagonal with space group P6/mmm [99].) In the type I and type II CHs, which we review here, the hydrogen-bonded H<sub>2</sub>O network combines to form three types of cages: pentagonal dodecahedron (D), tetrakaidecahedral (T), and hexakaidecahedral (H) which are shown in Fig. 12. The oxygen coordination is close to tetrahedral, i.e. the first-neighbor environment of each water molecule is similar to that in hexagonal and cubic ice. The type I unit cell is 12 Å and consists of 2 D-cages and 6 T-cages (46 water molecules) with average cage radiuses of, respectively, 3.95 Å and 4.33 Å [91]. The type II unit cell is 17 Å and consists of 16 D-cages and 8 H-cages (136 water molecules) with average cage radiuses of, respectively, 3.91 Å and 4.73 Å [91]. Dependent on sizes of "guest" molecules, these can accommodate the small, large or both type of cages in the type I and type II CHs.

The most commonly studied CH is probably THF CH, which crystallizes in the type II structure with the THF molecules accommodating the 8 H-cages, i.e. an ideal composition: THF·17 H<sub>2</sub>O (=136/8). It is known that THF CH decomposes on pressurization at relatively high temperatures [100,101,102] but below 140 K it instead amorphizes [93,96,97,103]. The decomposition at high temperatures occurs in gradual steps; the homogenous type II CH first transforms into ice and type I clathrate, THF·7 H<sub>2</sub>O, at 0.23 GPa, further to a state referred to as a non-clathrate hydrate (THF·5 H<sub>2</sub>O) at 0.53 GPa, and then finally into pure THF and ice well above 1.5 GPa [100]. (The transformation to the type I CH may also produce a mixture of amorphous material and ice phases [104].) Manakov *et al.* [105] has described this in a *p-T* phase diagram of THF CH.

During pressurization at low temperatures, the transition to the type I CH does not occur. This is likely due to sluggish kinetics in the same manner as a transition from hexagonal ice, ice Ih, to a high pressure ice is obstructed. Instead ice transforms to an amorphous state, high density amorphous ice (HDA), near 1 GPa on pressurization below about 140 K [10,106]. A similar effect was reported by Handa *et al.* [96] when CHs were pressurized at 77 K. They found transitions corresponding to that in ice Ih in the type II CHs: THF CH and SF<sub>6</sub> CH at 1.3 GPa and 1.6 GPa, respectively. However, they did not find a transition in a type I CH (Xe CH) up to the maximum pressure of 1.8 GPa. Moreover, on depressurization, the type II CH reverted (partially) to the original crystalline state. In a later study, Suzuki [93] improved the stability of the amorphized THF CH by annealing the collapsed state at 150 K and 1.5 GPa, and the state could thereafter be recovered at 77 K at atmospheric pressure to establish its amorphous nature. This effect of improved stability is likely similar to that which occurs when HDA ice is heated at pressures near 1 GPa. In the case of ice, it has been shown that the originally heterogeneous state, which is produced by pressurization to ~1.5 GPa at 77 K state homogenizes [107] and densifies on heating to ~150 K near 1 GPa, and the ultimately densified state is generally referred to as vHDA [108]. The treatment at high pressure and high temperature apparently removes inhomogeneous remnants

left after the collapse. In the case of THF CH, these remnants cause the recrystallization on depressurization of the collapsed state. In a recent study, Bauer *et al.* [109] showed that a carefully high-pressure annealed state could be heated to 150 K at atmospheric pressure before slow recrystallization into the type II CH commenced.

The thermal properties of type II CHs have been thoroughly studied down to low temperatures at both atmospheric pressure and elevated pressures. Fig. 13a shows the heat capacity for THF·16.64 H<sub>2</sub>O [110], THF·16.64 H<sub>2</sub>O doped with  $1.8 \cdot 10^{-4}$  mole fraction of KOH [110], and THF·16.65 H<sub>2</sub>O on cooling at 0.05 GPa [97]. (The latter was calculated from data for  $\rho c_p$  [97] and density [111,112]). As shown, the KOH-doped sample, but not the pure samples, displays a transition at low temperatures. This transition is the CH counterpart of the proton-ordering transition observed in KOH doped ice Ih [61,62,110]. Although the proton mobility is less restricted in CHs than in ice, which has been attributed to more defects in the CHs due to guest-water hydrogen bonding [90,113,114], it is still insufficient to induce a proton-ordering transition. That is, a dopant (e.g. KOH) is required to relax the ice rules [62] also in CHs, or else the transition to the thermodynamically more stable low-temperature proton-ordered state does not occur due to sluggish kinetics.

The thermal properties of CHs under high pressure was first studied by Ross and co-workers [21,94,95]. Their results for  $\kappa$  of DO·16.46·H<sub>2</sub>O (DO = 1,3-dioxolane), CB·16.50 H<sub>2</sub>O (CB = cyclobutanone) [95], and THF·16.59 H<sub>2</sub>O [94] at 0.1 GPa are shown in Fig. 13b. Fig. 13b also include results for KOH doped THF·16.9 H<sub>2</sub>O [115] and THF·16.9 D<sub>2</sub>O at 0.1 GPa [115], as well as atmospheric pressure results for THF CHs [116,117,118]. Ross *et al.* [21] originally suggested that the glass-like behavior of  $\kappa$  was due to phonon scattering caused by the reorientational motion of the guests, but it was later shown that CHs with monoatomic guests also displayed glass-like behavior. The results of Ross *et al.* (Fig. 13b) show that the magnitude of  $\kappa$  depends only weakly on the guest species. Moreover, the behavior of  $\kappa$  is also not much different whether or not the protons are ordered. The results for KOH-doped normal and deuterated THF CH [115] show that  $\kappa$  increases ca. 15% at the ordering transition near 62 K, and also that the glass-like behavior remains unchanged in the low-temperature proton-ordered phase. The increase at the transition, which is almost identical to that at the proton-ordering transition in ice Ih [119], can be accounted for by a decrease in the ice lattice anharmonicity. (A decrease, or vanishing, of scattering from a source would affect  $\kappa$  of ice Ih and CHs differently since  $\kappa$  of ice Ih is crystalline-like and about 10 times larger than that of CHs.)

If we turn to the effect of pressure on the thermal properties, then the most interesting is the change at the pressure collapse. The transition is unique in the sense that the CHs transforms from a crystalline phase with glass-like  $\kappa$  to a real glassy state, or at least an amorphous state. Fig. 14 shows the behavior of DO CH and THF CH during pressurization at about 130 K [97]. The  $\rho c_p$  data show a strong increase near 1 GPa, which is caused by densification and due to the collapse of the CHs. The behavior in the two different CHs is identical with about the same increase in  $\rho c_p$  during the collapse, but the data suggest that the lattice is slightly more stable with THF guests than with DO guests. The behavior in  $\kappa$  is more complex with an initial decrease before an abrupt increase. The decrease was attributed to a slight decrease in the phonon mean free path (Eq. 2) as the crystal lattice deforms and the empty cages in its structure begin to collapse [103], i.e. the decrease is a precursor of the major collapse. As the major collapse commences, the density increases significantly, and therefore also the phonon velocity and, accordingly,  $\kappa$ . An interesting comparison can be made using the density dependence of  $\kappa$ , or the Bridgman parameter  $g$  (see Eq. 6). This parameter has been estimated as 0.9 for THF CH [103], which corresponds to a  $\kappa$  increase of 27% for a 30% increase in density. The density increase at the collapse is roughly

30%, but the change in  $\kappa$  is only about 10%, i.e. 17% less than if the CHs would remain crystalline during the densification. Thus, although the  $\kappa$  behavior of the (crystalline) CHs is glass-like, the magnitude is still larger than that of a corresponding amorphous state of the same density. A similar comparison can be made at the melting point of the CHs. Measurements show that  $\kappa$  of the clathrate is about 15% higher than that of the melt, and in this case the density of the two states is about the same. Thus, the two independent calculations show that the melting or amorphization of the crystalline lattice at constant density causes a decrease of 15-17% in  $\kappa$ .

Data for  $\rho c_p$  of two collapsed CHs measured on heating at 1 GPa are depicted in Fig. 15 [97] together with those for the HDA ice (collapsed ice) and the as-made CH at 0.05 GPa. The behavior in  $\rho c_p$  of the collapsed states is identical showing an initial weak increase with temperature up to 140 K, of the same size as that for the crystalline, as-made, phase at 0.05 GPa. But at 140 K,  $\rho c_p$  of the collapsed states displays a stretched sigmoidal change, which is typical at a glass-liquid transition. The change is about the same in all the collapsed states and corresponds to a heat capacity increase of 3.7-3.9 J mol<sup>-1</sup> K<sup>-1</sup>. On further heating, collapsed ice crystallizes at about 154 K, whereas the collapsed CHs remain stable to significantly higher temperatures. These data show that there is an almost identical glass transition in collapsed ice and collapsed CHs under these conditions. The glass transition must therefore be associated with the H<sub>2</sub>O network, and the relatively large heat capacity step, which is larger than that observed for hyperquenched glassy water [120] and amorphous solid water at 1 atm [121], suggests that this is a glass to liquid transition. An orientational glass transition, which has been established in crystalline ices and CHs, shows a heat capacity step, which is typically less than 1 J (H<sub>2</sub>O-mol)<sup>-1</sup> K<sup>-1</sup> [110,122,123]. Still, further studies are required to fully establish that these transitions corresponds to glass-liquid transitions.

The behavior of the collapsed state is interesting as it appears to be a glassy state of a water solution with perfectly spaced solute molecules. Because of random fluctuations, such a state is impossible to achieve directly by vitrifying a liquid (water) solution. Moreover, water normally crystallizes unless the solute is strongly interacting, or in high concentration, and then the solute molecules are typically rejected into the ice grain boundaries. But in the case the water solution is a CH former, then crystallization instead distributes the solute molecules equidistantly in the crystal. After pressure collapse, this perfect distribution of the solute molecules remains and apparently obstructs formation of ice nuclei. Consequently, the collapsed state of CHs are less prone to crystallize to ice than similar water solutions vitrified by rapid cooling. Furthermore, THF, DO and other CH formers are relatively weakly interacting solutes compared to e.g. glycols, which are commonly used to study highly viscous water solutions. Thus this opens up for studies of ultraviscous water solutions with low concentrations of relatively weakly interacting solute molecules.

Recently, Tulk *et al.* [124] showed that also a type I CH of deuterated methane hydrate, CF<sub>4</sub>·6.26 D<sub>2</sub>O, collapses to amorphous state at 3.2 GPa during pressurization at 100 K, i.e. pressure collapse may be a general phenomenon of both type I and type II CHs, but with the collapse pressure being much higher for type I CHs. Moreover, Tulk *et al.*'s study [124] showed that the collapsed state was stable up to high temperatures, e.g. 220 K in the 1.5 GPa to 4 GPa range, which is significantly higher than for collapsed ice.

Other important findings in CHs under pressure concern new clathrate structures in the H<sub>2</sub>+H<sub>2</sub>O system, which is interesting for hydrogen storage applications [5]. H<sub>2</sub>+H<sub>2</sub>O mixtures form a type II clathrate at low pressures [125,126,127], which is stable up to 0.36 GPa. At high pressure, two new clathrates have been reported [128], and the phase diagram has been studied and summarized by Strobel *et al.* [129]. (Efimchenko *et al.* [130]

have shown that the  $p$ - $T$  diagram of the deuterated system,  $D_2+D_2O$ , is similar to that of the normal system at pressures below 0.18 GPa.) Moreover, Lokshin and Zhao have showed that clathrate formation in the  $H_2+H_2O$  system occurs much faster if ice is used as starting material instead of formation from water and hydrogen [131].

## SUMMARY AND CONCLUSIONS

In this review, we have mainly focused on the thermal conductivity of a number of inclusion compounds: hydroquinone, Dianin's compound, urea, thiourea, and clathrate hydrates, and their transition behaviors under high pressure. Several of these show remarkable differences in thermal conductivity behavior from that typically observed for crystalline species, but the reason for this deviant behavior remains unresolved. The summary here shows that high pressure studies may help resolving this issue. In particular, Dianin's compound, which is stable both with and without guest molecules, provides unique possibilities to study the effect of guest molecules on the thermal conductivity behavior. Studies at atmospheric pressure suggest that it has glass-like thermal conductivity both with and without guests [84,85] and, thus, that the behavior is not directly associated with guest molecules. This result instead advocates models which link the glass-like behavior indirectly to presence of guest molecules, e.g. a guest-induced change of (host) structure. Dharma-wardana [88] has presented such a model for clathrate hydrates, which ascribes the glass-like behavior to the large unit cell of clathrate hydrates, and the consequently numerous optical phonon modes. Recent results for La- and Ce-filled  $Fe_4Sb_{12}$  by Koza *et al.* [25] and  $Ba_8Ga_{16}Ge_{30}$  (type I clathrate) by Christensen *et al.* [26], which all show glass-like thermal conductivity, are also in conflict with the prevailing model of resonance scattering due to "rattling" guest motions. These studies instead suggest strong scattering by Umklapp processes and/or flat dispersion relations (low phonon velocity) for many of phonon modes. But since Umklapp scattering gives a thermal conductivity that varies as  $T^{-1}$ , this must be combined with another condition. For example, that the Umklapp scattering is sufficiently strong to quench the mean free path to its minimum possible value, or close to that value. These two studies provide results that are consistent with, but do not prove, the theoretical model of clathrate hydrates by Dharma-wardana.

Since results for the thermal conductivity of both empty and filled Dianin's compound under pressure is crystalline-like [83], it may be possible to directly observe changes that can explain the transformation from glass-like to crystalline-like behavior by studies of this compound on pressurization. For example, significant pressure induced changes in low-frequency vibrational modes, which can serve as phonon scatters, and/or acoustic phonon modes, may explain the reduced scattering at high pressure. In order for the results to be consistent with the model of Dharma-wardana, should require the finding of a structural transition at pressures below that for crystalline-like behavior, i.e. below or near 0.035 GPa [83].

We also note that the thermal conductivity behavior of hydroquinone inclusion compound is unknown and that the  $\beta$ -form may be studied both with and without guests, but that the latter is metastable against the  $\alpha$ -form. Again, this provides an important possibility to gain further information about the glass-like thermal conductivity. Moreover, the summary of the studies of the phase diagram of hydroquinone has revealed an unresolved issue concerning the transition behavior on pressurization at room temperature. Structural studies [46,47] do not support findings of a transition, which has been reported to occur near 3.3 GPa [44]. However, thermal studies at high temperatures and low pressures show a phase transition with negative temperature-pressure phase line [42]. That is, if these results are extended to high pressures, it is possible to resolve whether or not the  $\alpha$ -form of hydroquinone show a (first or second order) transition at 3.3 GPa to a new structural form.

The combined results of the thermal and Raman properties suggest that hydroquinone has a structural form with unknown structure, the  $\delta$ -form, which is stable both near 1 atm at high temperatures, and at room temperature and high pressures.

Finally, we find that clathrate hydrates may provide possibilities to obtain glassy and ultraviscous states of water solutions in which the solute molecules are perfectly spaced. This perfect distribution of solute molecules occurs when a water solution of a clathrate hydrate former crystallize on cooling, and it should remain when the clathrate hydrate collapses to an amorphous state on pressurization at low temperatures. Due to random fluctuation in a liquid, it seems difficult to obtain such a state by rapid cooling of liquid solutions and, in particular, water solutions.

#### **ACKNOWLEDGEMENTS**

This work was supported financially by the Swedish Research Council, and by the Faculty of Science and Technology, Umeå University. O.A. acknowledges financial support for equipment from Carl Trygger Foundation and Magn. Bergvalls foundation.

## REFERENCES AND NOTES

- [1] Weber E.; Josel, H.-P. A proposal for the classification and nomenclature of host-guest-type compounds. *J. Inc. Phenom.*, **1983**, *1*, 79-85.
- [2] According to the IUPAC Gold Book, an inclusion compound is “A complex in which one component (the host) forms a cavity or, in the case of a crystal, a crystal lattice containing spaces in the shape of long tunnels or channels in which molecular entities of a second chemical species (the guest) are located. There is no covalent bonding between guest and host, the attraction being generally due to van der Waals forces. If the spaces in the host lattice are enclosed on all sides so that the guest species is 'trapped' as in a cage, such compounds are known as clathrates or 'cage compounds'.”  
McNaught, A.D.; Wilkinson, A. *Compendium of Chemical Terminology* ("The Gold Book") 2<sup>nd</sup> ed.; Blackwell Scientific Publications: Oxford, 1997. <http://goldbook.iupac.org/I02998.html>
- [3] Slack, G. A.; Tsoukala, V. G. Some properties of semiconducting IrSb<sub>3</sub>. *J. Appl. Phys.*, **1994**, *76*, 1665–1671.
- [4] Takabatake, T.; Suekuni, K.; Nakayama, T.; Kaneshita, E. *Phonon-glass electron-crystal thermoelectric clathrates: Experiments and theory*. Review of Modern Physics. 2014
- [5] Struzhkin, V. V.; Militzer, B.; Mao, W. L.; Mao, H.-K.; Hemley, R. J. Hydrogen storage in molecular clathrates. *Chem. Rev.*, **2007**, *107*, 4133–4151.
- [6] Parsonage, N. G.; Staveley, L. A. K. *Disorder in Crystals*; Oxford: Clarendon, **1978**.
- [7] Belosludov, V. R.; Laverentiev, M. Y.; Dyadin, Y. A. Theory of clathrates. *J. Inclusion Phenom.* **1991**, *10*, 399-422.
- [8] English N. J.; Tse J. S. Perspectives on hydrate thermal conductivity. *Energies*, **2010**, *3*, 1934-1942.
- [9] Yamamuro, O.; Suga, H. Thermodynamic studies of clathrate hydrates. *J. Therm. Anal. Calorim.* **1989**, *35*, 2025-2064.
- [10] Mishima, O.; Calvert, L. D.; Whalley, E. An apparently first-order transition between two amorphous phases of ice induced by pressure. *Nature*, **1985**, *314*, 76–78.
- [11] Huang, C.; Wikfeldt, K. T.; Tokushima, T.; Nordlund, D.; Harada, Y.; Bergmann, U.; Niebuhr, M.; Weiss, T. M.; Horikawa Y.; Leetmaa, M.; Ljungberg, M. P.; Takahashi, O.; Lenz, A.; Ojamäe, L.; Lyubartsev, A. P.; Shin, S.; Pettersson, L. G. M.; Nilsson, A. The inhomogeneous structure of water at ambient conditions. *Proc. Natl. Acad. Sci. USA*, **2009**, *106*, 15214–15218.
- [12] Andersson, O.; Inaba, A. Thermal conductivity of crystalline and amorphous ices and its implications on amorphization and glassy water. *Phys. Chem. Chem. Phys.* **2005**, *7*, 1441–1449.
- [13] Maglič, K. D.; Cezairliyan, A.; Peletsky, V. E. *Compendium of thermophysical property measurement methods*, Vol. 1 *Survey of Measurement Techniques*; Plenum Press: New York, London, **1984**.
- [14] Bäckström, G. Thermophysical properties of solids under *high pressure* (a review). *High Temp. - High Pressures*, **1985**, *17*, 185-199.
- [15] Goncharov, A. F.; Wong, M.; Dalton, D. A.; Ojwang, J. G. O.; Struzhkin, V. V.; Konôpková, Z.; Lazor, P. Thermal conductivity of argon at high pressures and high temperatures. *J. Appl. Phys.*, **2012**, *111*, 112609 (6 pages).
- [16] Carslaw, H. S.; Jaeger, J. C. *Conduction of heat in solids* 2<sup>nd</sup> ed.; Clarendon: Oxford, **1959**, pp. 341.
- [17] Andersson, O.; Sundqvist, B.; Bäckström, G. A low-temperature high-pressure *apparatus with a temperature control system*. *High Press. Res.* **1992**, *10*, 599-606.
- [18] Andersson, O. Simulation of a glass transition in a hot-wire experiment using time-dependent heat capacity. *Int. J. Thermophys.*, **1997**, *18*, 195–208.
- [19] Berman, R. Thermal Conductivity of Glasses at Low Temperatures. *Phys. Rev.*, **1949**, *76*, 315-316.
- [20] Tonpheng, B.; Andersson, O. Crosslinking, thermal properties and relaxation behavior of polyisoprene under high-pressure. *Eur. Polym. J.* **2008**, *44*, 2865-2873.
- [21] Ross R. G.; Andersson P.; Bäckström, G. Unusual *PT* dependence of thermal conductivity for a clathrate hydrate. *Nature*, **1981**, *290*, 322-323.
- [22] Tse, J. S.; White, M. A. Origin of glassy crystalline behavior in the thermal properties of clathrate hydrates: a thermal conductivity study of tetrahydrofuran hydrate. *J. Phys. Chem.*, **1988**, *92*, 5006-5011.
- [23] Slack, G. A. In *CRC Handbook of Thermoelectrics*; Rowe, D. M., Ed.; CRC Press: Boca Raton, 1995; p. 407–440.
- [24] Tse, J. S.; Klug, D. D.; Zhao, J. Y.; Sturhahn, W.; Alp, E. E.; Baumert, J.; Gutt, C.; Johnson, M. R.; Press, W. Anharmonic motions of Kr in the clathrate hydrate. *Nat. Mater.* **2005**, *4*, 917–921.

- [25] Koza, M. M.; Johnson, M. R.; Viennois, R.; Mutka, H.; Girard, L.; Ravot, D. Breakdown of phonon glass paradigm in La- and Ce-filled Fe<sub>4</sub>Sb<sub>12</sub> skutterudites. *Nat. Mater.*, **2008**, *7*, 805–810.
- [26] Christensen, M.; Abrahamsen, A. B.; Christensen, N. B.; Juranyi, F.; Andersen, N. H.; Lefmann, K.; Andreasson, J.; Bahl, C. R. H.; Iversen, B. B. Avoided crossing of rattler modes in thermoelectric materials. *Nat. Mater.*, **2008**, *7*, 811–815.
- [27] Roufosse, M.; Klemens, P. G. Thermal Conductivity of Complex Dielectric Crystals. *Phys. Rev. B*, **1973**, *7*, 5379-5386.
- [28] Andersson, O.; Suga, H. Thermal conductivity of amorphous ices. *Phys. Rev. B*, **2002**, *65*, 140201 (4 pages).
- [29] Berman, R. *Thermal conduction in solids*. Clarendon: Oxford, **1976**.
- [30] Parrot, J. E.; Stuckes, A. D. *Thermal conductivity of solids*. Pion Limited: London, **1975**.
- [31] Andersson, S. P.; Andersson, O.; Bäckström, G. Thermal conductivity of amorphous Teflon (af 1600) at high pressure. *Int. J. Thermophys.*, **1997**, *18*, 209-219.
- [32] Yamamuro, O.; Oguni, M.; Matsuo, T.; Suga, H. Heat capacity measurements under high pressure. *Thermochim. Acta*, **1988**, *123*, 73–83.
- [33] Umehara, I.; Hedo, M.; Tomioka, F.; Uwatoko, Y. Heat capacity measurements under high pressure. *J. Phys. Soc. Jpn.*, **2007**, *76*, 206-209.
- [34] Matsubayashi, K.; Hedo, M.; Umehara, I.; Katayama, N.; Ohgushi, K.; Yamada, A.; Munakata, K.; Matsumoto, T.; Uwatoko, Y. High-pressure ac specific heat technique with cubic anvil apparatus. *J. Phys.: Conf. Ser.*, **2010**, *215*, 012187 (4 pages).
- [35] Derr, J.; Knebel, G.; Lapertot, G.; Salce, B.; Méasson, M.-A.; J. Flouquet, J. Valence and magnetic ordering in intermediate valence compounds: TmSe versus SmB<sub>6</sub>. *J. Phys.: Condens. Matter*, **2006**, *18*, 2089–2106.
- [36] Wallwork, S. C.; Powell, H. M. The crystal structure of the  $\alpha$ -form of quinol. *J. Chem. Soc., Perkin Trans. 2*, **1980**, 641-646.
- [37] Maartmann-Moe, K. The crystal structure of  $\gamma$ -hydroquinone. *Acta Crystallogr.*, **1966**, *21*, 979-982.
- [38] Nam, B.-U.; Kim, B.-S.; Lee, H.-H.; Yoon, J.-H. Structural transformation and guest dynamics of methanol-loaded hydroquinone clathrate observed by temperature-dependent raman spectroscopy. *J. Phys. Chem. A*, **2012**, *116*, 2435–2438.
- [39] Palin, D. E.; Powell, H. M. The structure of molecular compounds. Part VI. The  $\beta$ -type clathrate compounds of quinol. *J. Chem. Soc.*, **1948**, 815-821.
- [40] Palin, D. E.; Powell, H. M. The structure of molecular compounds. Part III. Crystal structure of addition complexes of quinol with certain volatile compounds. *J. Chem. Soc.* **1947**, 208–221.
- [41] Lindeman, S.V.; Shklover, V.E.; Struchkov, Yu.T. The beta-modification of hydroquinone, C<sub>6</sub>H<sub>6</sub>O<sub>2</sub>. *Cryst. Struct. Commun.*, **1981**, *10*, 1173-1179.
- [42] Naoki, M.; Yoshizawa, T.; Fukushima, N.; Ogiso, M.; Yoshino, M. A new phase of hydroquinone and its thermodynamic properties. *J. Phys. Chem. B*, **1999**, *103*, 6309-6313.
- [43] Timmermans, J. Plastic crystals: A historical review. *J. Phys. Chem. Solids*, **1961**, *18*, 1-8.
- [44] Rao, R.; Sakuntala, T.; Arora, A. K.; Deb, S. K. Pressure induced phase transitions in hydroquinone. *J. Chem. Phys.*, **2004**, *121*, 7320–7325.
- [45] Tse, J. S. Mechanical instability in ice I h. A mechanism for pressure induced amorphization. *J. Chem. Phys.*, **1992**, *96*, 5482-5487.
- [46] Lee, Y.; Lee, J.-W.; Lee, H.-H.; Lee, D.-R.; Kao, C.-C.; Kawamura, T.; Yamamoto, Y.; Yoon, J.-H. High pressure investigation of  $\alpha$ -form and CH<sub>4</sub>-loaded  $\beta$ -form of hydroquinone compounds. *J. Chem. Phys.*, **2009**, *130*, 124511 (6 pages).
- [47] Kim, B.-S.; Lee, Y.; Yoon, J.-H. Pressure-dependent release of guest molecules and structural transitions in hydroquinone clathrate. *J. Phys. Chem. B*, **2013**, *117*, 7621–7625.
- [48] Matsuo, T.; Suga, H.; Seki, S. Phase transitions in the quinol clathrate compounds. I. The quinol hydrogen cyanide clathrate compound. *J. Phys. Soc. Jpn.*, **1971**, *30*, 785-793.
- [49] Matsuo, T. Phase transitions in the quinol clathrate compounds. II. The quinol methanol clathrate compound. *J. Phys. Soc. Jpn.*, **1971**, *30*, 794-805.
- [50] Harris, K. D. M. Fundamental and applied aspects of urea and thiourea inclusion compounds. *Supramol. Chem.* **2007**, *19*, 47–53.
- [51] Bridgman, P. W. Polymorphism at high pressures. *Proc. Am. Acad. Arts Sci.*, **1916**, *52*, 91-187.
- [52] Bridgman, P. W. Polymorphic transitions up to 50,000 kg/cm<sup>2</sup> of several organic substances. *Proc. Am. Acad. Arts Sci.*, **1938**, *72*, 227-268.
- [53] Hamann, S. D.; Linton, M. Infrared spectra and phase transitions of solids under pressure. Part 1. *High Temp. High Press.*, **1975**, *7*, 165-175.
- [54] Weber, H.-P.; Marshall, W. G.; Dmitriev, V. High-pressure polymorphism in deuterated urea. *Acta Crystallogr., Sect. A*, **2002**, *58*, 174 (1 page).

- [55] Marshall, W. G.; Francis, D. J. Attainment of near-hydrostatic compression conditions using the Paris-Edinburgh cell. *J. Appl. Crystallogr.*, **2002**, *35*, 122–125.
- [56] Swaminathan, S.; Craven, B. M.; McMullan, R. K. The crystal structure and molecular thermal motion of urea at 12, 60 and 123 K from neutron diffraction. *Acta Crystallogr., Sect. B*, **1984**, *40*, 300–306.
- [57] Olejniczak, A.; Ostrowska, K.; Katrusiak, K. H-bond breaking in high-pressure urea. *J. Phys. Chem. C*, **2009**, *113*, 15761–15767.
- [58] Birkedal, M.; Madsen, D.; Mathiesen, R.; Knudsen, K.; Weber, H.-P.; Pattison, P.; Schwarzenbach, D. The charge density of urea from synchrotron diffraction data. *Acta Crystallogr., Sect. A*, **2004**, *60*, 371–381.
- [59] Andersson, O.; Ross, R. G. Phase behavior and thermal conductivity of urea at pressures up to 1 GPa and at temperatures in the range 50–370 K. *Int. J. Thermophys.*, **1994**, *15*, 513–524.
- [60] Andersson, O.; Matsuo, T.; Suga, H.; Ferloni, P. Low-temperature heat capacity of urea. *Int. J. Thermophys.*, **1993**, *14*, 149–158.
- [61] Tajima, Y.; Matsuo, T.; Suga, H. Phase transition in KOH-doped hexagonal ice. *Nature*, **1982**, *299*, 810–812.
- [62] The proton motions in ice I are restricted by the ‘ice rules’ in the tetrahedrally coordinated ice structure; each of the four bonds exhibits two proton sites and, according to the ice rules, these are occupied so that there are two protons adjacent to each oxygen and one proton on each bond. This imposes strong limitations on the proton mobility and the necessity of defects, such as Bjerrum defects, vacancies, and grain boundaries, for H<sub>2</sub>O reorientational relaxation.
- [63] Bonin, M.; Marshall, W. G.; Weber, H.-P.; Toledano, F. Annual Report 1998; ISIS Pulsed Neutron and Muon Source, Rutherford Appleton Laboratory: Didcot, U.K., **1998**; pp 34-35. <http://www.isis.rl.ac.uk/>.
- [64] Ross, R. G.; Andersson, P.; Sundqvist, B.; Bäckström, G. Thermal conductivity of solids and liquids under pressure. *Rep. Prog. Phys.*, **1984**, *47*, 1347–1402.
- [65] Smith, A. E. The crystal structure of the urea-hydrocarbon complexes. *Acta Crystallogr.*, **1952**, *5*, 224–235.
- [66] Harris, K. D. M.; Thomas, J. M. Structural aspects of urea inclusion compounds and their investigation by X-ray diffraction: a general discussion. *J. Chem. Soc. Faraday Trans.*, **1990**, *86*, 2985–2996.
- [67] Toudic, B.; Rabiller, P.; Bourgeois, L.; Huard, M.; Ecolivet, C.; McIntyre, G. J.; Bourges, P.; Brezowski, T.; Janssen, T. Temperature-pressure phase diagram of an aperiodic host guest compound. *Europhys. Lett.*, **2011**, *93*, 16003 (5 pages).
- [68] Ross, R. G. Thermal conductivity of the urea-hexadecane inclusion compound. *J. Inclusion Phenom. Mol. Recog. Chem.*, **1990**, *8*, 227–233.
- [69] Pemberton, R. C.; Parsonage, N. G. Thermodynamic properties of urea+hydrocarbon adducts. Part 1.—Heat capacities of the adducts of n-C<sub>10</sub>H<sub>22</sub>, n-C<sub>12</sub>H<sub>26</sub>, n-C<sub>16</sub>CH<sub>34</sub> and n-C<sub>20</sub>H<sub>42</sub> from 12 to 300°K. *Trans. Faraday Soc.*, **1965**, *61*, 2112–2121.
- [70] Andersson, O.; Ross, R. G.; Bäckström, G. Thermal conductivity of crystalline and glassy crystal cyclohexanol under pressure. *Mol. Phys.*, **1989**, *66*, 619–635.
- [71] Handa, Y.P.; Cook, J.G. Thermal Conductivity of Xenon Hydrate. *J. Phys. Chem.*, **1987**, *91*, 6327–6328.
- [72] Krivchikov, A. I.; Gorodilov, B. Y.; Korolyuk, O. A.; Manzhelii, V. G.; Romantsova, O. O.; Conrad, H.; Press, W.; Tse, J. S.; Klug, D. D. Thermal conductivity of Xe clathrate hydrate at low temperatures. *Phys. Rev. B*, **2006**, *73*, 064203 (6 pages).
- [73] Leonidva, G. Ferroelectric properties of thiourea under high pressures. *G. Fiz. Tverd. Tela* **1963**, *5*, 3430 (translation: *Sov. Phys. Solid State* **1964**, *5*, 2519).
- [74] Gesi, K. J. Effect of hydrostatic pressure on phase transitions in thiourea. *J. Phys. Soc. Jpn.* **1969**, *26*, 107–112.
- [75] Figuiere, P.; Ghelfenstein, M.; Szwarc, H. First-order phase diagram of thiourea and Raman spectroscopy. *Chem. Phys. Lett.* **1975**, *33*, 99–103.
- [76] Menon, C. P.; Philip, J. Thermal properties of thiourea studied using photopyroelectric technique. *Ferroelectrics*, **2003**, *287*: 63–70.
- [77] Bilski, P.; Czarnecki, P.; Lewicki, S.; Wasicki, J. The p–T phase diagram for ferroelectric bis-thiourea pyridinium nitrate. *J. Chem. Thermodynamics*, **2011**, *43*, 1211–1214.
- [78] Bilski, P.; Bobrowicz-Sarga, L.; Czarnecki, P.; Marczak, A.; Wasicki, J. The p–T phase diagram for new ferroelectric bis-thiourea pyridinium bromide. *J. Chem. Thermodynamics*, **2013**, *59*, 182–187.
- [79] Abriel, W.; du Bois, A.; Zakrzewski, M.; White, M. A. The crystal structure and thermal expansion of the CCl<sub>4</sub> adduct of Dianin's compound. *Can. J. Chem.*, **1990**, *68*, 1352–1356.
- [80] Flippin, J. L.; Karle, J.; Karle, I. L. Crystal structure of a versatile organic clathrate. 4-p-Hydroxyphenyl-2,2,4-trimethylchroman (Dianin's compound). *J. Am. Chem. Soc.*, **1970**, *92*, 3749–3755.
- [81] Imashiro, F.; Yoshimura, M.; Fujiwara, T. 'Guest-free' Dianin's compound. *Acta Crystallogr., Sect. C: Cryst. Struct. Commun.*, **1998**, *54*, 1357–1360.

- [82] Lee, J. J.; Sobolev, A. N.; Turner, M. J.; Fuller, R. O.; Iversen, B. B.; Koutsantonis, G. A.; Spackman, M. A. Molecular imprisonment: Host response to guest location orientation and dynamics in clathrates of Dianin's compound. *Cryst. Growth Des.*, **2014**, *14*, 1296–1306.
- [83] Andersson, O.; Murashov, V.; White, M. A. Thermal conductivity and heat capacity of dianin's clathrates under pressure. *J. Phys. Chem. B*, **2002**, *106*, 192-196.
- [84] Zakrzewski, M.; White, M. A. Thermal conductivities of a clathrate with and without guest molecules. *Phys. Rev. B*, **1992**, *45*, 2809-2817.
- [85] Michalski, D.; M.A. White, M. A. Thermal conductivity of a clathrate with restrained guests: the CCl<sub>4</sub> clathrate of Dianin's compound. *J. Phys. Chem.*, **1995**, *99*, 3774-3780.
- [86] Murashov, V. V.; White, M. A. Apparatus for dynamical thermal measurements of low-thermal diffusivity particulate materials at subambient temperatures. *Rev. Sci. Instrum.* **1998**, *69*, 4198-4204.
- [87] R. I. Beecroft, R. I.; Swenson, C. A. Behavior of polytetrafluoroethylene (Teflon) under high pressures. *J. Appl. Phys.* **1959**, *30*, 1793–1798.
- [88] Dharma-Wardana, M. W. C. The thermal conductivity of the ice polymorphs and the ice clathrates. *J. Phys. Chem.*, **1983**, *87*, 4185–4190.
- [89] Andersson, O.; Chobal, O.; Rizak, I.; Rizak, V.; Sabadosh, V. Effects of pressure and temperature on the thermal conductivity of Sn<sub>2</sub>P<sub>2</sub>S<sub>6</sub>. *Phys. Rev. B*, **2011**, *83*, 134121 (7 pages).
- [90] Davidson, D. W. Clathrate Hydrates. In *Water — A Comprehensive Treatise*; Franks, F., Ed.; Plenum: New York, **1973**; Vol. 2, Chapter 3, p 115.
- [91] Sloan E.D. *Clathrate Hydrates of Natural Gas*. 2nd ed.; Dekker: New York, 1998.
- [92] Slack, G. A. In: *Solid State Physics* ; Ehrenreich, H.; Seitz, F.;Turnbull D. Eds. ; Academic: New York, **1979**; Vol. 34, pp. 1-71.
- [93] Suzuki, Y. Evidence of pressure-induced amorphization of tetrahydrofuran clathrate hydrate. *Phys. Rev. B*, **2004**, *70*, 172108 (4 pages).
- [94] Ross, R. G.; Andersson, P. Clathrate and other solid phases in the tetrahydrofuran-water system: thermal conductivity and heat capacity under pressure. *Can. J. Chem.*, **1982**, *60*, 881-892.
- [95] Andersson P.; Ross, R. G. Effect of guest molecule size on the thermal conductivity and heat capacity of clathrate hydrates. *J. Phys. C: Solid State Phys.*, **1983**, *16*, 1423-1432.
- [96] Handa, Y. P.; Tse, J. S.; Klug, D. D.; Whalley, E. Pressure-Induced Transitions in Clathrate Hydrates. *J. Chem. Phys.*, **1991**, *94*, 623–627.
- [97] Andersson, O.; Inaba, A. Glass transitions in pressure-collapsed ice clathrates and implications for cold water. *J. Phys. Chem. Lett.*, **2012**, *3*, 1951–1955.
- [98] Amann-Winkel K.; Gainaru, C.; Handle, P. H.; Seidl, M.; Nelson, H.; Böhmer, R.; Loerting, T. Water's second glass transition.. *Proc. Natl. Acad. Sci. U.S.A.*, **2013**, *110*, 17720–17725.
- [99] Ripmeester, J. A.; Tse, J. S.; Ratcliffe, C. I.; Powell, B. M. A new clathrate hydrate structure. *Nature*, **1987**, *325*, 135–136.
- [100] Manakov, A. Yu.; . Goryainov, S. V.; Likhacheva, A. Yu.; Fursenko, B. A.; Dyadina, Y. A.; Kurnosov, A. V. High-pressure boundary of hydrate formation in the tetrahydrofuran–water system. *Mendeleev Commun.*, **2000**, *10*, 80–81.
- [101] Dyadin, Yu. A.; Bondaryuk I. V.; Zhurko, F. V. *Clathrate Hydrates at High Pressures*. In: *Inclusion Compounds*; eds. Atwood, J. L.; Davies, J. E. D.; MacNicol, D. D. Eds.; Oxford University Press: Oxford, **1991**; vol. 5, 213-275.
- [102] Dyadin, Yu, A.; Kuznetsov, P. N.; Yakovlev, I. I.; Pyrinova, A. V. The system water-tetrahydrofuran in the crystallization region at pressures of up to 9 kbar. *Doklady. Chem.*, **1973**, *208*, 9–12.
- [103] Andersson, O.; Johari, G. P. Collapse of an ice clathrate under pressure observed via thermal conductivity measurements. *Phys. Rev. B*, **2008**, *78*, 174201. (9 pages)
- [104] Zakrzewski, M.; Klug, D. D.; Ripmeester, J. A. On the Pressure-Induced Phase Transformation in the Structure II Clathrate Hydrate of Tetrahydrofuran. *J. Inclusion Phenom.* **1994**, *17*, 237-247.
- [105] Manakov, A. Yu.; Goryainov, S. V.; Kurnosov, A. V. Likhacheva, A. Yu.; Dyadina, Y. A.; Larionov, E. G. Clathrate nature of the high-pressure tetrahydrofuran hydrate phase and some new data on the phase diagram of the tetrahydrofuran-water system at pressures up to 3 GPa. *J. Phys. Chem. B*, **2003**, *107*, 7861-7866.
- [106] Mishima, O. Reversible first-order transition between two H<sub>2</sub>O amorphs at ~0.2 GPa and ~135 K. *J. Chem. Phys.* , **1994**, *100*, 5910-5912.
- [107] Koza, M.M.; Hansen, T.; May, R.P.; Schober, H. Link between the diversity, heterogeneity and kinetic properties of amorphous ice structures. *J. Non Cryst. Solids*, **2006**, *352*, 4988–4993.
- [108] Loerting, T.; Salzmann, C.; Kohl, I.; Mayer, E.; Hallbrucker, A. A second distinct structural “state” of high-density amorphous ice at 77 K and 1 bar. *Phys. Chem. Chem. Phys.*, **2001**, *3*, 5355–5357.
- [109] Bauer, M.; Töbrens, D. M.; Mayer, E.; Loerting, T. Pressure-amorphized cubic structure II clathrate hydrate: Crystallization in slow motion. *Phys. Chem. Chem. Phys.*, **2011**, *13*, 2167–2171.

- [110] Yamamuro, O.; Oguni, M.; Matsuo, T.; Suga, H. Calorimetric study of pure and KOH-doped tetrahydrofuran clathrate hydrate. *J. Phys. Chem. Solids*, **1988**, *49*, 425-434.
- [111] Gough, S. R.; Davidson, D. W. Composition of tetrahydrofuran hydrate and the effect of pressure on the decomposition. *Can. J. Chem.*, **1971**, *49*, 2691-2699.
- [112] Hester, K. C.; Huo, Z.; Ballard, A. L.; Koh, C. A.; Miller, K. T.; Sloan, E. D. Thermal expansivity for sI and sII clathrate hydrates. *J. Phys. Chem. B*, **2007**, *111*, 8830-8835.
- [113] Alavi, S.; Susilo, R.; Ripmeester, J. A. Linking microscopic guest properties to macroscopic observables in clathrate hydrates: Guest-host hydrogen bonding. *J. Chem. Phys.*, **2009**, *130*, 174501 (9 pages).
- [114] Nelson, H.; Schildmann, S.; Nowaczyk, A.; Gainaru, C.; Geil, B.; Böhmer, R. Small-angle water reorientations in KOH doped hexagonal ice and clathrate hydrates. *Phys. Chem. Chem. Phys.*, **2013**, *15*, 6355-6367.
- [115] Andersson, O.; Suga, H. Thermal conductivity of normal and deuterated tetrahydrofuran clathrate hydrates. *J. Phys. Chem. Solids*, **1996**, *57*, 125-132.
- [116] Krivchikov, A. I.; Manzhelii, V. G.; Korolyuk, O. A.; Gorodilov, B. Ya.; Romantsova, O. O. Thermal conductivity of tetrahydrofuran hydrate. *Phys. Chem. Chem. Phys.*, **2005**, *7*, 728-730.
- [117] Ashworth, T.; Johnson, L. R.; Lai, L.-P. Thermal conductivity of pure ice and tetrahydrofuran clathrate hydrates. *High Temp. High Pressures*, **1985**, *17*, 413-419.
- [118] Cook, J. G.; Laubitz, M. J. In *Thermal Conductivity*; Hust, J. G., Ed.; Plenum Press: New York, **1983**, Vol. 17, p 745-751.
- [119] Andersson, O.; Suga, H. Thermal-conductivity of the Ih and XI phases of ice. *Phys. Rev. B*, **1994**, *50*, 6583-6588.
- [120] Johari, G. P.; Hallbrucker, A.; Mayer, E. The glass-liquid transition of hyperquenched water. *Nature*, **1987**, *330*, 552-553.
- [121] Hallbrucker, A.; Mayer, E.; Johari, G. P. Glass-liquid transition and the enthalpy of devitrification of annealed vapor-deposited amorphous solid water. A comparison with hyperquenched glassy water. *J. Phys. Chem.*, **1989**, *93*, 4986-4990.
- [122] Haida, O.; Matsuo, T.; Suga, H.; Seki, S. Relaxational Proton Ordering and Glassy Crystalline State in Hexagonal Ice. *Proc. Jpn. Acad.*, **1972**, *48*, 489-494.
- [123] Haida, O.; Matsuo, T.; Suga, H.; Seki, S. Calorimetric study of the glassy state X. Enthalpy relaxation at the glass-transition temperature of hexagonal ice. *J. Chem. Thermodyn.*, **1974**, *6*, 815-825.
- [124] Tulk, C. A.; Klug, D. D.; Molaison, J. J.; dos Santos, A. M.; Pradhan, N. Structure and stability of an amorphous water-methane mixture produced by cold compression of methane hydrate. *Phys. Rev. B*, **2012**, *86*, 054110 (8 pages).
- [125] Dyadin, Y. A.; Larionov, E. G.; Manakov, A. Y.; Zhurko, F. V.; Aladko, E. Y. Clathrate hydrates of hydrogen and neon. *Mendeleev Commun.*, **1999**, *5*, 209-210.
- [126] Dyadin, Y. A.; Larionov, E. G.; Aladko, E. Y.; Manakov, A. Y.; Zhurko, F. V.; Mikina, T. V.; Komarov, V. Y.; Grachey, E. V. Clathrate formation in water-noble gas (hydrogen) systems at high pressures. *J. Struct. Chem.*, **1999**, *40*, 790-795.
- [127] Mao, W. L.; Mao, H. K.; Goncharov, A. F.; Struzhkin, V. V.; Gou, Q. Z.; Hu, J. Z.; Shu, J. F.; Hemley, R. J.; Somayazulu, M.; Zhao, Y. S. Hydrogen clusters in clathrate hydrate. *Science*, **2002**, *297*, 2247-2249.
- [128] Vos, W. L.; Finger, L. W.; Hemley, R. J.; Mao, H. K. Novel H<sub>2</sub>-H<sub>2</sub>O clathrates at high pressures. *Phys. Rev. Lett.*, **1993**, *71*, 3150-3153.
- [129] Strobel, T. A.; Somayazulu, M.; Hemley, R. J. Phase behavior of H<sub>2</sub> + H<sub>2</sub>O at high pressures and low temperatures. *J. Phys. Chem. C*, **2011**, *115*, 4898-4903.
- [130] Efimchenko, V. S.; Antonov, V. E.; Barkalov, O. I.; Klyamkin, S. N. Temperature-pressure phase diagram of a D<sub>2</sub>O-D<sub>2</sub> system at pressures to 1.8 kbar. *J. Phys. Chem. B*, **2008**, *112*, 7026-7031.
- [131] Lokshin, K. A.; Zhao, Y. Fast synthesis method and phase diagram of hydrogen clathrate hydrate. *Appl. Phys. Lett.*, **2006**, *88*, 131909 (3 pages).

---

## Figure Captions

Fig. 1. Sample cell made of Teflon for measurements of thermal properties using the hot-wire method under pressure [12]. The hot-wire is heated by a short current pulse and the thermal properties of the surrounding sample are obtained through an analysis of the temperature rise of the wire using Eq. (1).

Fig. 2. Phase diagram of hydroquinone under pressure. The dashed lines represent conjectured extensions of the phase boundary between the  $\alpha$ -form and the  $\delta$ -form (unknown structure), which is established below 0.1 GPa [42]. The filled circle with lines (error boundaries) represent the transition pressure of a transition suggested in a Raman study [44]. The inset shows the chemical structure of hydroquinone.

Fig. 3. Phase diagram of urea. Dashed lines represent the phase lines reported by Bridgman [51,52]. Crosses represent phase transitions obtained for a commercially pure sample and the solid line represents results for a carefully purified urea sample [59]. The inset shows the chemical structure of urea.

Fig. 4. Transition behaviour of urea. (a) Heat capacity per unit volume and (b) thermal conductivity plotted against pressure at the temperatures indicated. (c) Heat capacity per unit volume and (d) thermal conductivity plotted against temperature at the pressures indicated [59]. (Results for heat capacity affected by the phase I to III transition were removed to avoid confusion [59].)

Fig. 5. Phase diagram of fully deuterated urea-nonadecane inclusion compound [67]. The shaded range indicates a metastable region “between phases II and III, on the one hand, and the phase IV, on the other hand.” [67].

Fig. 6. Thermal and transition properties of urea-hexadecane. (a) Thermal conductivity measured on cooling and heating at 0.1 GPa [68]. (b) Thermal conductivity of urea (phase I) [59] and urea-hexadecane inclusion compound.

Fig. 7. Phase diagram of thiourea after Gesi [74]. The inset shows the chemical structure of thiourea.

Fig. 8. Thermal conductivity of thiourea plotted as a function of temperature at 1 atm [76]. The results were measured along different crystal axes for a single crystal. Note the unit, which is the same as in the original publication [76], i.e.  $\text{W cm}^{-1} \text{K}^{-1}$ .

Fig. 9. Phase diagrams of two thiourea inclusion compounds: (a) bis-thiourea pyridinium nitrate [77] and (b) bis-thiourea pyridinium bromide [78]. (The dashed lines show discontinuous transition, whereas the black solid lines show continuous transitions.) For bis-thiourea pyridinium nitrate, Bilski *et al.* [77] wrote “For pressures up to 450 MPa, the transition between the ferroelectric and paraelectric phases (III-II phase) is continuous, whereas above 450 MPa, the phase transition between these phases (III-I phase) is discontinuous.” For bis-thiourea pyridinium bromide, Bilski *et al.* [78] concluded “The transition from phase I to II is continuous and that from phase III to IV is discontinuous, while that from phase II to III is discontinuous for pressure up to about 300 MPa and continuous above 300 MPa.”

---

Fig. 10. Thermal properties of Dianin's compound. (a) Heat capacity per unit volume at 0.2 GPa (no data at 1 atm or at 0.15 GPa) and (b) thermal conductivity at the pressures indicated plotted against temperature (labels in 10a). The results refer to both single crystal data (Dianin's compound without guests at 1 atm) and polycrystalline data (the other data sets). The results were obtained using the hot-wire method (HW) and steady-state radial heat flow method (RHF) under pressure [83], and modulated heat flow method (MHF) at 1 atm [84,85,86].

Fig. 11. (a) Heat capacity per unit volume and (b) thermal conductivity plotted against pressure for Dianin's compound with  $\text{CCl}_4$  guest molecules.

Fig. 12. The three structures showing the oxygen positions in the three cages (not to scale), which build the CH structures; from left to right: pentagonal dodecahedron (D, 12 pentagonal faces -  $5^{12}$ ) with a cage radius of  $\sim 3.9$  Å, tetrakaidecahedral (T,  $5^{12}6^2$ ) with a cage radius of  $\sim 4.3$  Å, and hexakaidecahedral (H,  $5^{12}6^4$ ) with a cage radius of  $\sim 4.7$  Å.

Fig. 13 (a) Molar heat capacities for tetrahydrofuran (THF) clathrate hydrates: pure and KOH doped THF·16.64  $\text{H}_2\text{O}$  [110] and THF·16.65  $\text{H}_2\text{O}$  (calculated from data for  $\rho c_p$  at 0.05 GPa [97] and density [111, 112] at 1 atm). (b) Thermal conductivity for: DO·16.46· $\text{H}_2\text{O}$  (DO = 1,3-dioxolane), CB·16.50  $\text{H}_2\text{O}$  [95] (CB = cyclobutanone), THF·16.59  $\text{H}_2\text{O}$  [94], THF·16.9  $\text{H}_2\text{O}$  [115], THF·16.9  $\text{D}_2\text{O}$  [115] at 0.1 GPa; and THF·16.9  $\text{H}_2\text{O}$  [116], THF·16  $\text{H}_2\text{O}$  [117], and THF·17  $\text{H}_2\text{O}$  [118] at 1 atm.

Fig. 14. (a) Heat capacity per unit volume and (b) thermal conductivity plotted as a function of pressure at 130 K for: 1,3 dioxolane (DO) and tetrahydrofuran (THF) type II clathrate hydrates. The abrupt changes near 1 GPa are due to collapse of the crystalline structure.

Fig. 15. Heat capacity per unit volume of collapsed states at 1 GPa, and as-made THF CH at 0.05 GPa.

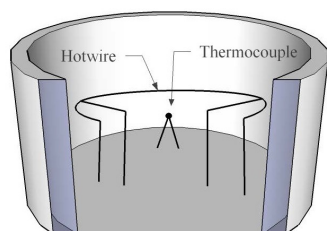


Figure 1.

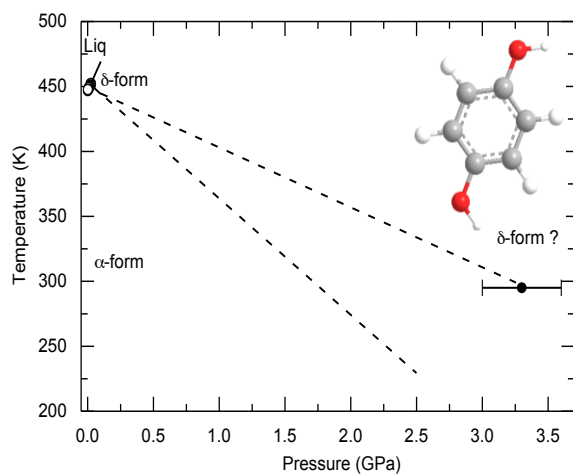


Figure 2.

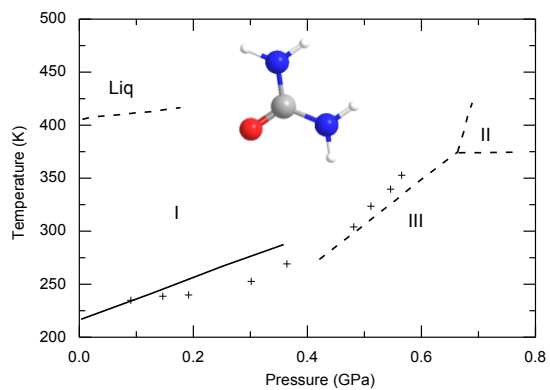


Figure 3.

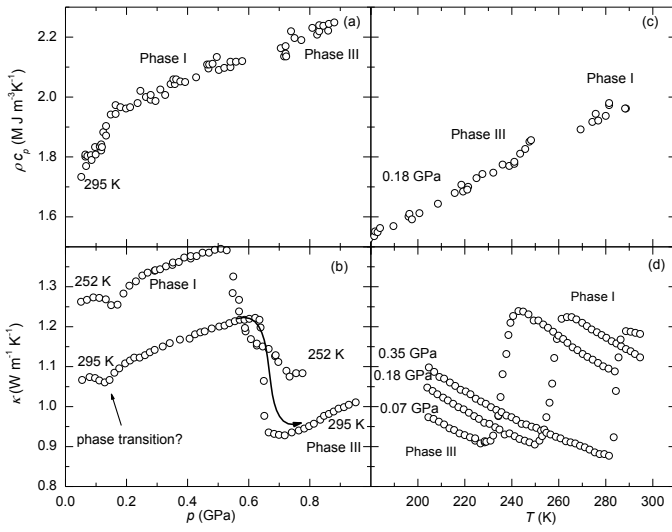


Figure 4.

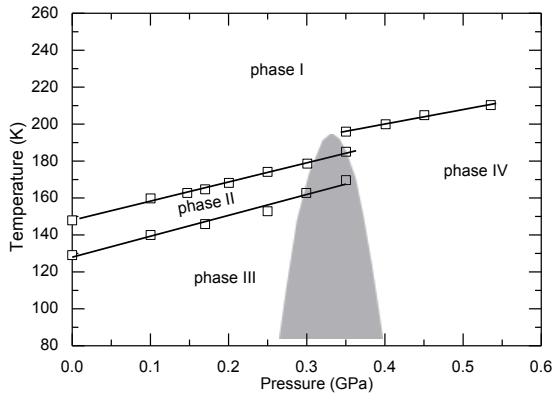


Figure 5.

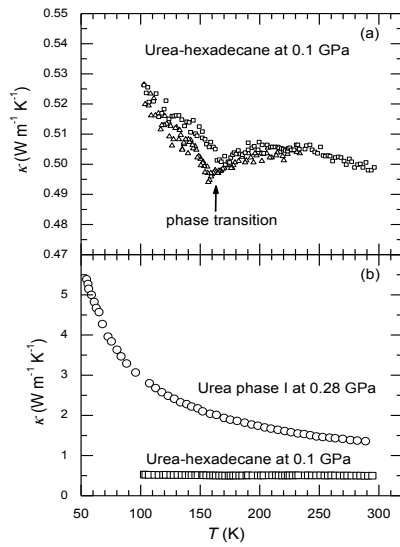


Figure 6.

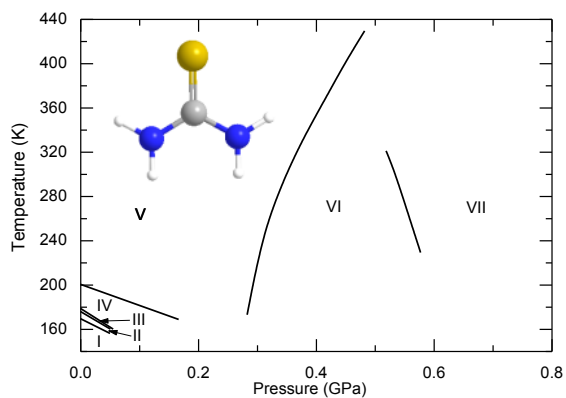


Figure 7.

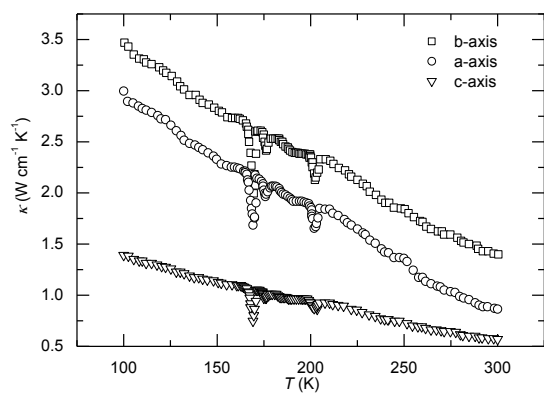


Figure 8.

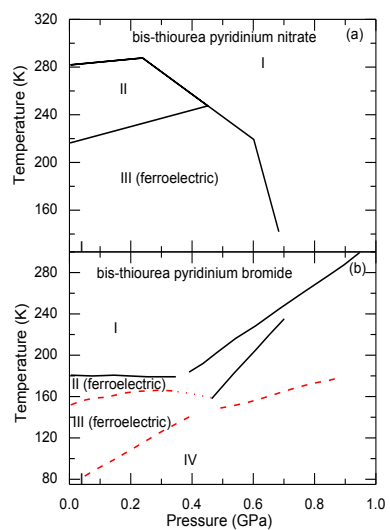


Figure 9.

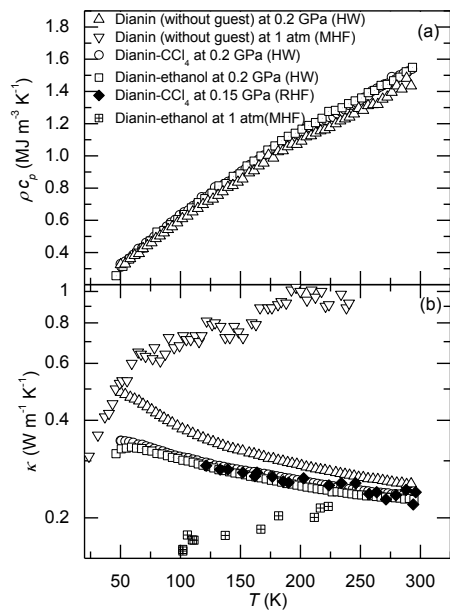


Figure 10.

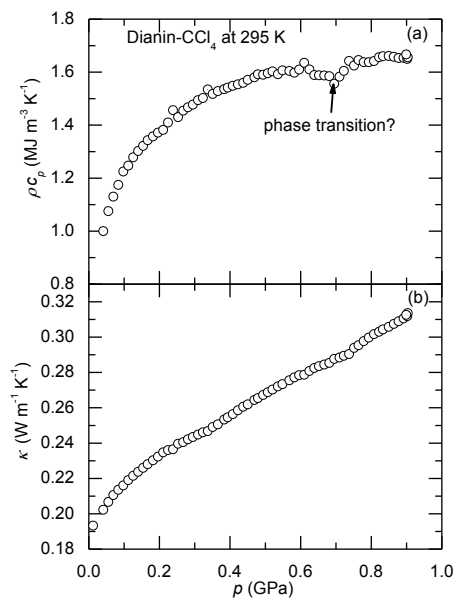


Figure 11.

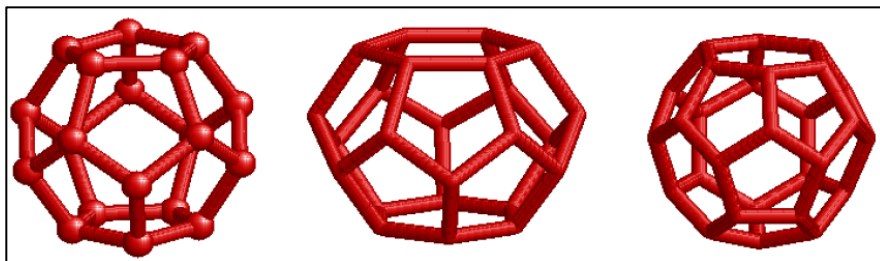


Figure 12.

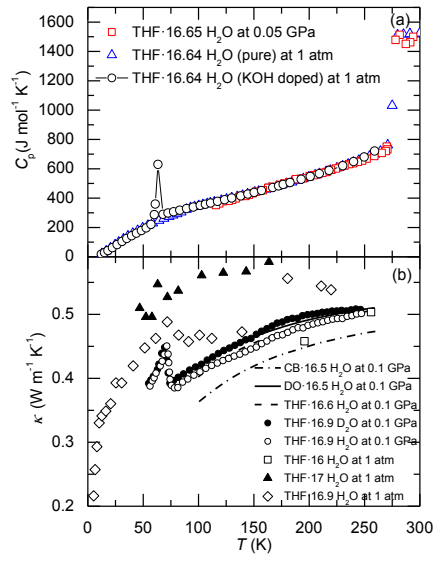


Figure 13.

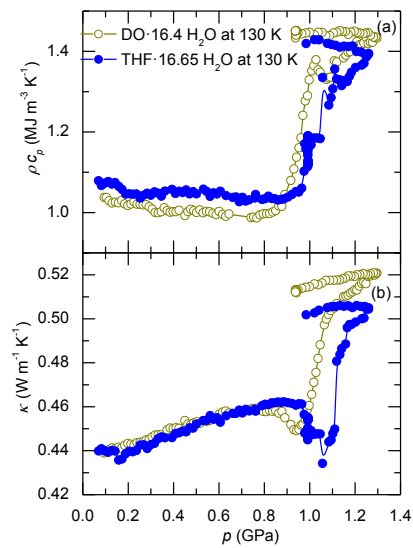


Figure 14.

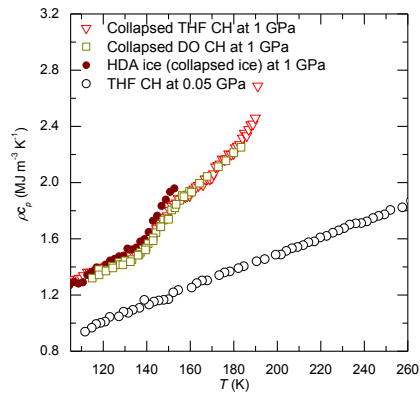


Figure 15.